Journal of Medicinal Chemistry

pubs.acs.org/jmc

Drug Annotation

Discovery of OATD-01, a First-in-Class Chitinase Inhibitor as Potential New Therapeutics for Idiopathic Pulmonary Fibrosis

Robert Koralewski, Barbara Dymek, Marzena Mazur, Piotr Sklepkiewicz, Sylwia Olejniczak, Wojciech Czestkowski, Krzysztof Matyszewski, Gleb Andryianau, Piotr Niedziejko, Michal Kowalski, Mariusz Gruza, Bartłomiej Borek, Karol Jedrzejczak, Agnieszka Bartoszewicz, Elżbieta Pluta, Aleksandra Rymaszewska, Magdalena Kania, Tomasz Rejczak, Sylwia Piasecka, Michal Mlacki, Marcin Mazurkiewicz, Michał Piotrowicz, Magdalena Salamon, Agnieszka Zagozdzon, Agnieszka Napiorkowska-Gromadzka, Aneta Bartlomiejczak, Witold Mozga, Paweł Dobrzański, Karolina Dzwonek, Jakub Golab, Marcin Nowotny, Jacek Olczak, and Adam Golebiowski*

Cite This: https://dx.doi.org/10.1021/acs.jmedchem.0c01179

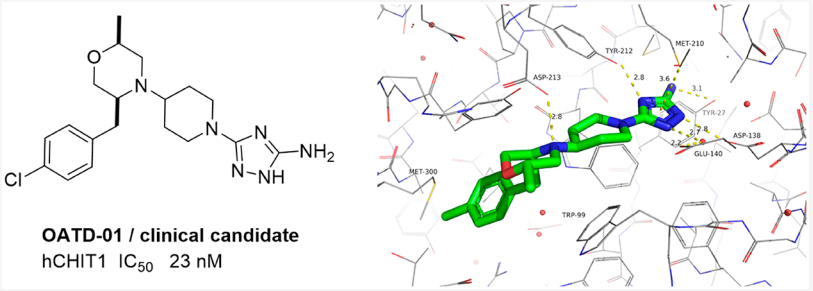

ABSTRACT: Chitotriosidase (CHIT1) and acidic mammalian chitinase (AMCase) are the enzymatically active chitinases that have been implicated in the pathology of chronic lung diseases such as asthma and interstitial lung diseases (ILDs), including idiopathic pulmonary fibrosis (IPF) and sarcoidosis. The clinical and preclinical data suggest that pharmacological inhibition of CHIT1 might represent a novel therapeutic approach in IPF. Structural modification of an advanced lead molecule **3** led to the identification of compound **9** (**OATD-01**), a highly active CHIT1 inhibitor with both an excellent PK profile in multiple species and selectivity against a panel of other off-targets. **OATD-01** given orally once daily in a range of doses between 30 and 100 mg/kg showed significant antifibrotic efficacy in an animal model of bleomycin-induced pulmonary fibrosis. **OATD-01** is the first-in-class CHIT1 inhibitor, currently completed phase 1b of clinical trials, to be a potential treatment for IPF.

INTRODUCTION

Chitinases are chitin-degrading enzymes that belong to the glycosyl hydrolase family 18, which includes enzymatically active chitinases and chitinase-like proteins without enzymatic activity.[1−3] Mammals have two distinct genes encoding for chitinase enzymes, chitotriosidase (*CHIT1*) and acidic mammalian chitinase (*CHIA*, hereafter referred to as AMCase).[4] Both enzymes are composed of a catalytic domain linked by a flexible hinge to chitin binding domain belonging to the carbohydrate-binding module family 14. The catalytic domain shows a conserved cluster of three acidic residues in its active-site cleft that are involved in the reaction of chitin hydrolysis. The highly conserved chitin binding domain facilitates recognition of crystal chitin.[5] Both enzymes were shown to modulate inflammatory response in chitin-dependent and -independent manner. While AMCase is mostly produced at sites of Th2 inflammation and modulates allergic response in animal models of asthma,[6−8] CHIT1 was reported to be the main chitinase produced by tissue activated macrophages[3,9−11] and expressed in human lung[12] and liver.[13−15] Moreover, CHIT1 was shown to modulate TGFβ and IL-13 signaling pathways to promote fibrotic response in animal models of pulmonary fibrosis.[16]

Currently, most antifibrotic treatment strategies are limited to specific diseases or organs. More evidence demonstrates great similarities among inflammatory and fibroproliferative diseases, and new drugs are being shown to be effective antifibrotic therapies across different diseases and organs.[17]

Received: July 7, 2020

CHIT1 is having a wide spectrum of scientific and clinical interest mostly due to its specific localization in chronically activated tissue macrophages that infiltrate the lungs of patients suffering from chronic lung diseases, such as severe asthma,[9,18−20] progressive fibrotic interstitial lung diseases (ILDs), such as idiopathic pulmonary fibrosis (IPF)[16,21] or sarcoidosis,[21−23] and chronic obstructive pulmonary disease (COPD).[9,18,24] However, pathological tissue macrophages that highly express CHIT1 are found also in liver disorders such as nonalcoholic steatohepatitis (NASH) or hepatic fibrosis and cirrhosis in general suggesting their role in liver diseases that progress to fibrosis.[14]

IPF is a devastating and rapidly progressing fibroproliferative lung disease, with an estimated 5-year survival of approximately 20%, characterized by epithelial damage, fibroproliferative matrix deposition, and parenchymal remodeling.[25−28] Despite pirfenidone and nintedanib being approved for the treatment of IPF, these compounds show moderate efficacy in delaying the lung functional decline and disease progression. IPF is still a greatly unmet medical need; therefore the search for new therapeutic targets to support existing treatments is highly demanded.

Activated profibrotic tissue macrophages[29] are thought to be the drivers of fibrosis in IPF lungs. Intriguingly, CHIT1 is the only chitinase induced in activated macrophages in vitro[3,9,12,17] and found to be one of the markers of profibrotic macrophages in IPF lungs. Initial studies evaluating the role of CHIT1 in the pathogenesis of pulmonary fibrosis in mice showed that CHIT1 deficiency resulted in decreased pulmonary fibrosis by significant modulation of TGF-β- and IL-13-driven fibrotic responses.[16] This suggests a critical role of chitinases in the development of airway and interstitial fibrotic remodeling and implicates that pharmacological inhibition of CHIT1 is an attractive approach for patients suffering from fibrotic lung diseases.[30,31]

In addition, CHIT1 was suggested to facilitate tissue remodeling processes in fibroblastic liver tissue (similar to the lung) being produced by liver-specific macrophages, Kupffer cells, which by activating hepatic stellate cells induce hepatic fibrosis and cirrhosis.[14,15] Higher activity of CHIT1 has been also detected in the sera of patients with chronic hepatitis C virus (HCV) infection as compared to control individuals but most importantly also in the sera of patients with more pronounced fibrosis or liver cirrhosis as compared to patients with no or minimal liver fibrosis.[14,32,33] This significant correlation between serum CHIT1 and histological fibrosis stages or liver stiffness further underlines the important role of CHIT1 along with senescence for liver fibrogenesis.[32,34]

In the current studies we demonstrate discovery and development of a selective chitinase inhibitor **OATD-01** with low nanomolar activity toward CHIT1, exhibiting exceptional PK profile in multiple animal species. Furthermore, we confirmed antifibrotic properties of **OATD-01** in pulmonary interstitial fibrosis model induced by bleomycin.

RESULTS AND DISCUSSION

The main goal of our studies was to develop a chitinase inhibitor for the treatment of inflammation-driven fibrotic diseases. We searched for a molecule with single-digit nanomolar activity toward CHIT1, excellent PK/PD profile, and therapeutic activity in preclinical animal models of chronic pulmonary inflammation and fibrosis.

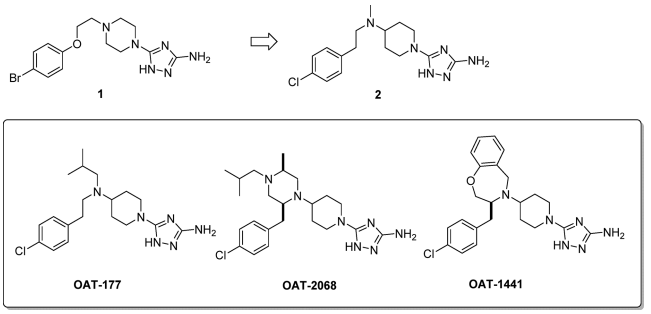

Our early research on chitinases inhibitors started from natural product, allosamidin, cyclic peptides,[35] and the literature reported molecule **1** (also called Wyeth 1),[36] which was optimized into an advanced lead compound **2**.[20] The initial SAR development led to improvement of in vitro activity by optimizing interactions with Asp213 (mostly by shifting scaffold design from the central piperazine ring into 4-aminopiperidine) and by further exploring hydrophobic interactions to gain selectivity toward murine (m) mAMCase (e.g., **OAT-177**),[20] human (h) hAMCase (e.g., **OAT-1441**),[37] and mCHIT1 (e.g., **OAT-2068**) (Table 1).[38] For the future clinical candidate, we decided to focus our work on hCHIT1/hAMCase inhibitors and progress lead compound **3**.[39] The independent, very recent publication on m- and hCHIT1 selective inhibitor and its antifibrotic activity in bleomycin induced lung fibrosis model in mice was reported by Jiang et al.[40]

Molecule **3**, compared to many others made in the program (>3K chitinase inhibitors have been synthesized and tested), has a unique in vitro profile, being a very strong inhibitor of all four isoforms of key chitinase targets, i.e., both mouse and human CHIT1 and AMCase. It also has a very good PK profile in both mice and rats, but its main liability is relatively high activity against dopamine transporter (DAT IC_{50} = 370 nM). This off-target effect was not surprising considering that the phenethylamine substructure (also present in all monoamines) can be easily found in the compound **3**. We have seen this off-target activity in some other of our early inhibitors, e.g., **OAT-177** (DAT 95% inhibition at 10 μM).[19]

In the first step, we have studied chitinase inhibition activity of other ring analogs of molecule **3**, e.g., compounds **4**−**8**. Piperidine series (represented by compound **4**) were as active as morpholines but with higher activity against hERG and monoamine transporters (likely because of higher basicity of the nitrogen atom in piperidines vs morpholines). Other replacements of the oxygen atoms (compounds **5**−**8**) proved to be inferior, with piperazine **6** being the most promising lead molecule. Further development of the SAR of compound **6** led to a higher mCHIT1 selectivity at the cost of activity against human enzymes, and although it gave an interesting tool molecule, i.e., mCHIT1 selective inhibitor **OAT-2068**,[38] it was later discontinued.

Alkyl substitution at position 2 of the morpholine ring, i.e., molecules **9**−**17**, turned out to be a suitable modification instantly abrogating activity toward dopamine transporter. This result represents the classic case of SAR-cliff or "magic methyl" discovery.[43−45] The cis-diasteroisomer **9** turned out to be a synthetically preferred isomer over the trans compound **10**,[46] with coincident higher activity against chitinases. Increasing the size of the 2-substituent (e.g., compounds **11**−**17**) led in general to equipotent inhibitors but with much inferior PK (e.g., compounds **11**, **15**, **16**, **17**; see Supporting Information).

https://dx.doi.org/10.1021/acs.jmedchem.0c01179
J. Med. Chem. XXXX, XXX, XXX−XXX

Table 1. Structure−Activity Relationship of Selected Analogs of Compound 3[a]

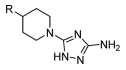

Cmpd #	R	hCHIT1 (IC_{50} nM)	mCHIT1 (IC_{50} nM)	hAMCase (IC_{50} nM)	mAMCase (IC_{50} nM)	hERG[b] (IC_{50} μM)	DAT[c]
OAT-177	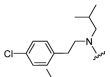	232 ± 48	2955 ± 50	14.2 ± 1.0	18.8 ± 0.4	4.0	95%
OAT-2068	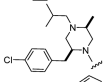	1250 ± 71	29 ± 4	84 ± 1.4	4170 ± 42	2.4	NT[d]
OAT-1441	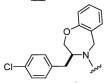	915 ± 85	137 ± 3.5	7.0 ± 2.0	59 ± 2.1	22	37%
3	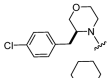	48 ± 8.2	74 ± 13.4	22 ± 2.1	30 ± 12.7	39	95%
4	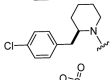	41 ± 8.5	87 ± 7.8	23 ± 2.1	81 ± 12	8.3	NT
5	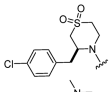	4200 ± 990	1700 ± 280	850 ± 0.0	3000 ± 71	NT	NT
6	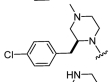	18000 ± 4900	1600 ± 0.0	400 ± 110	7600 ± 570	IA	3%
7	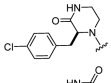	IA	27000 ± 5000	6400 ± 71	22000 ± 3500	NT	NT
8	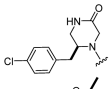	1400 ± 350	5300 ± 780	1300 ± 210	660 ± 140	80	12%
9 OATD-01	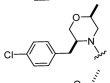	23 ± 4.5	28 ± 3.4	9.0 ± 1.0	7.8 ± 1.2	23	IA[d]
10	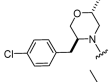	5100 ± 140	7200 ± 1100	830 ± 91	1000 ± 99	NT[d]	NT[d]
11	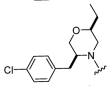	14 ± 0.7	14 ± 0.7	54 ± 11	1.3 ± 0.1	33	NT[d]
12	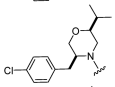	18 ± 0.7	19 ± 2.8	3.4 ± 0.5	2.1 ± 0.1	34	34%
13	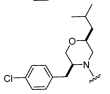	16 ± 2.3	15 ± 0.7	1.6 ± 0.1	1.0 ± 0.6	8.5	28%
14	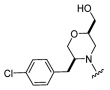	22 ± 0.7	25 ± 3.5	6.8 ± 0.3	6.7 ± 0.6	72	NT[d]
15	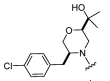	23 ± 0.6	29 ± 5.7	7.0 ± 2.5	5.5 ± 1.6	IA[d]	1%
16	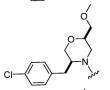	22 ± 3.5	30 ± 5.7	8.9 ± 0.3	7.7 ± 1.5	100	4%
17	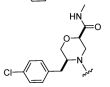	32 ± 6.4	49 ± 1.4	24 ± 4.2	7.8 ± 0.6	IA[d]	8

[a] IC_{50} data of each compound were determined in 2−3 independent assays, and mean IC_{50} ± SD values are shown in the table. [b] Data from Predictor hERG fluorescence polarization assay[41] [c] % inhibition at 10 μM. Data from DAT human dopamine transporter binding (antagonist radioligand) assay, Cerep.[42] [d] NT = not tested; IA = inactive.

Thus, compound **9** (**OATD-01**) was selected for further studies. To thoroughly determine its affinity toward h/mCHIT1 and h/mAMCase, the inhibitory constants (K_i) for all four enzymes have been measured and revealed good correlation with earlier established IC_{50} data (hCHIT1 K_i = 17.3 ± 11.3 nM; mCHIT1 K_i = 26.05 ± 7.7 nM; hAMCase K_i = 4.8 ± 1.3 nM; mAMCase K_i = 5.7 ± 4.1 nM; n = 3). Off-target in vitro effects of compound **OATD-01** have been evaluated at 10 μM in the Eurofins Panlabs panel of 98 in vitro binding and enzymatic assays, involving diverse molecular classes of proteins. These studies demonstrated no significant interactions as no inhibition or stimulation higher than 50% was observed. Similarly, no significant inhibition was observed in the panel of seven CYPs and 13 transporters (see Supporting Information for details).

An X-ray crystallography approach was used to gain insights into the structure of the hCHIT1−**OATD-01** complex and to understand the increased activity of the compound toward recombinant hCHIT1 in comparison with the previously reported **OAT-177**.[20] **OATD-01** was cocrystallized with the catalytic domain of hCHIT1. The obtained crystals belong to space group $P2_12_12_1$ and diffracted X-rays to 1.5 Å resolution at a synchrotron source. The hCHIT1−**OATD-01** complex structure was solved by molecular replacement, using the hCHIT1 structure (PDB code 1WB0) as the search model.

The **OATD-01** inhibitor occupies the chitin-binding cleft of hCHIT1 (Figure 1). The binding mode is largely the same as previously observed for the **OAT-177** compound. Two of the hCHIT1 catalytic triad residues (Asp136, Asp138, Glu140) bind the **OATD-01** aminotriazole ring by direct (Asp138, 2.8 Å) and water-mediated (Glu140) hydrogen bonds. In the apo structure (PDB code 4WJX) the side chain of Asp138 adopts two conformations, but in the presence of **OATD-01** is stabilized through a hydrogen bond with Asp136. The position of the carbonyl group of one of the alternative conformations of Asp138 in apo protein, in the inhibitor complex structure, is occupied by a water molecule mediating the Glu140−inhibitor interaction. The aminotriazole moiety is also directly H bonded to Tyr212 (2.7 Å) and Tyr27 (3.1 Å). The position of the ring is stabilized by van der Waals interactions with Met210, Met356, Trp358, Tyr27, and Ala183. Strong interaction between carboxylic group of the conserved catalytic Asp213 and nitrogen of the central ring of the inhibitor is crucial for the potency of inhibitors toward hCHIT1 and AMCase. As for compound **OAT-177**, 4-aminopiperidine core of the **OATD-01** forms stable hydrogen bond of 2.8 Å with Asp213.

The key difference between **OAT-177** and **OATD-01** is the presence of the 2-methylmorpholine ring. The analysis of the X-ray structure reveals why the inhibitor's activity is modified by the addition of the ring. First, the interactions between the inhibitor and Arg269 residue are altered (compare superimposition of the active site residues in hCHIT1 complexed to **OATD-01** and **OAT-177**; Supporting Information Figure 1). In the **OAT-177** complex the side chain of this residue adopts two alternative conformations, while in complex with **OATD-01** Arg269 has one conformation and forms van der Waals interactions with the 2-methylmorpholine ring (3.3−4.0 Å). Second, O03 oxygen and C04 carbon of the ring form van der Waals interactions with the side chain of Met300.

Similar to **OAT-177**, the 4-chlorobenzyl part of **OATD-01** occupies a hydrophobic pocket formed by Leu362, Ala302, Leu301, Tyr267, and Met300 residues. All of these residues form van der Waals interactions with of **OATD-01**. Chloride atom, located deep in the hydrophobic cavity, interacts with Thr295 within 3.6 Å distance. It was shown[20] that this interaction is key for inhibition of AMCase and CHIT1

https://dx.doi.org/10.1021/acs.jmedchem.0c01179
J. Med. Chem. XXXX, XXX, XXX−XXX

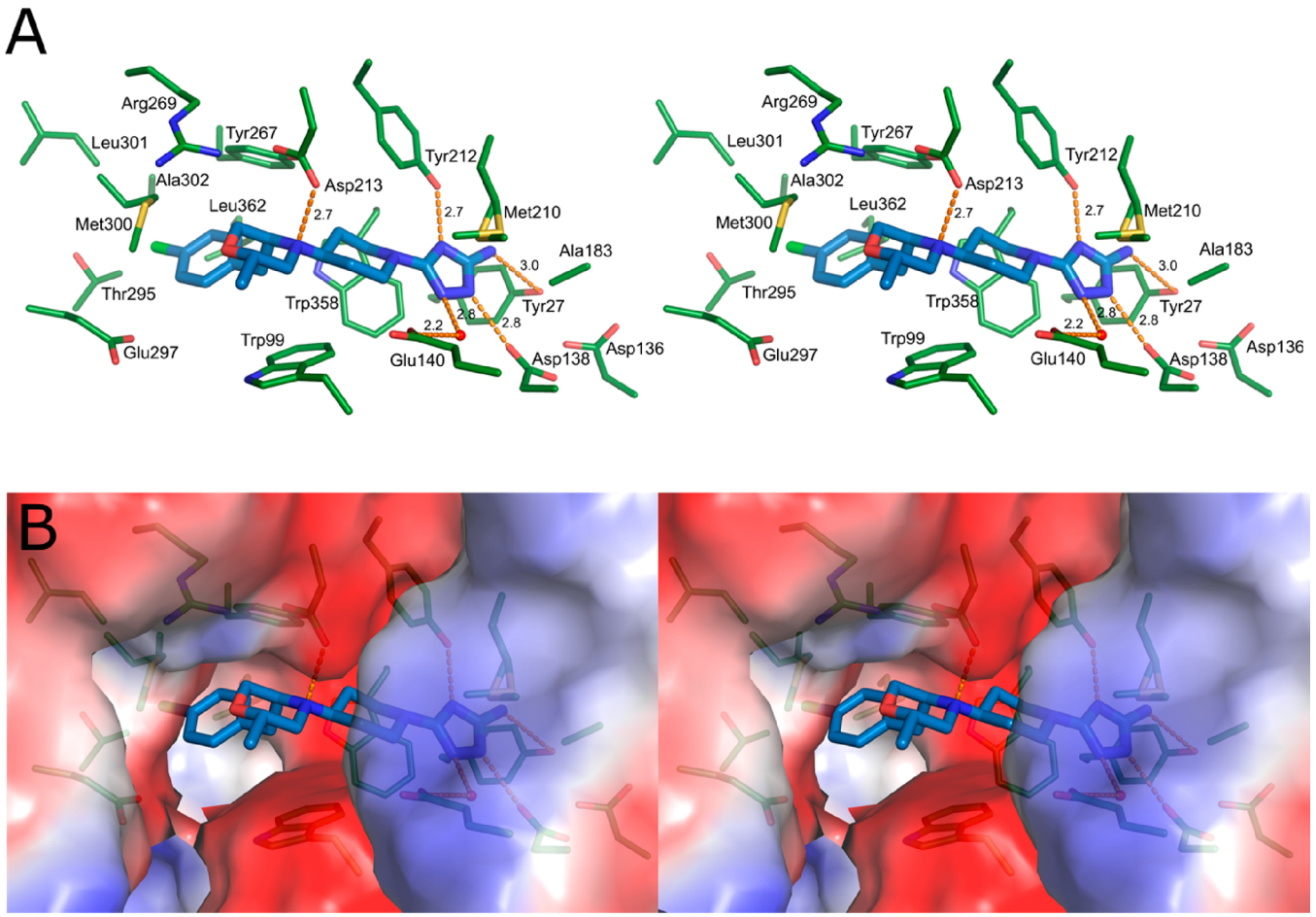

Figure 1. Structure of **OATD-01**−hCHIT1 complex (PDB code 6ZE8). The structure was solved by molecular replacement, using the hCHIT1 structure (PDB code 1WB0) as the search model. (A) Stereoview of key residues (shown as green sticks) of hCHIT1 active site. **OATD-01** compound is shown as blue sticks, water molecule as red sphere. Protein−ligand hydrogen bonds are represented by orange dashed lines, and distances are given in Å. (B) Stereoview of active site pocket of hCHIT1 represented as surface and colored according to electrostatic potential. Key residues of hCHIT1 active site are shown as green sticks. **OATD-01** compound is shown as blue sticks and water molecule as red sphere.

Scheme 1. Synthesis of OATD-01[a]

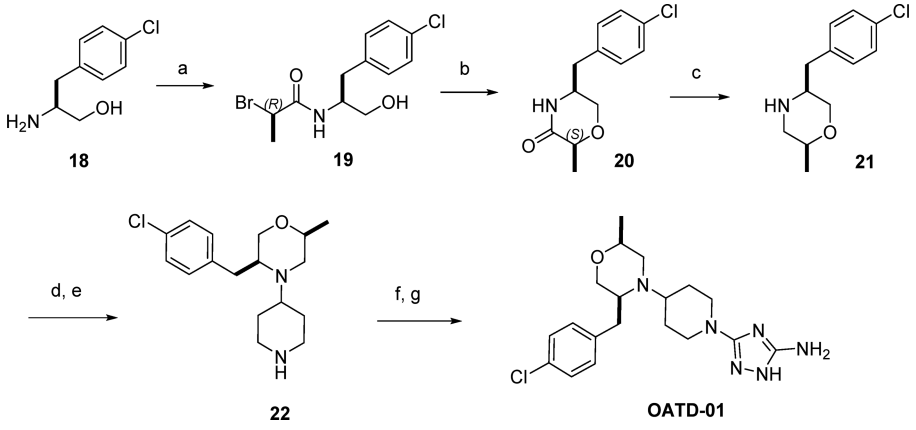

[a]Reagents and conditions: (a) (*R*)-2-bromopropionic acid, TBTU; CH_2Cl_2, rt, 60−80%; (b) NaH; THF, rt, 60−80%; (c) BH_3·DMS; THF, reflux, 60−80%; (d) *N*-Boc-piperid-4-one, $NaBH(OAc)_3$; DCE, AcOH, rt, 50−60%; (e) HCl(g); AcOEt, rt, 90%; (f) *S*,*S*′-dimethyl *N*-cyanodithioiminocarbonate, K_2CO_3; MeCN, reflux; (g) hydrazine; MeCN, reflux; ∼80% over two steps.

chitinases activity. Chitin-binding cleft is closed by Trp99 residue. The orientation of Trp99 is the same as that observed for **OAT-177** compound. Trp99 side chain forms van der Waals interactions with the 2-methyl group of morpholine, and 4-aminopiperidine thus plays a key role in stabilizing the overall conformation and strengthening the inhibitor binding.

OATD-01 was synthesized in several different ways, and its early preparation was carried out in the seven steps synthetic

https://dx.doi.org/10.1021/acs.jmedchem.0c01179
J. Med. Chem. XXXX, XXX, XXX−XXX

sequence (Scheme 1). Amino alcohol **18**[39] was acylated using optically active (*R*)-2-bromopropionic acid, and the intermediate **19** was subsequently cyclized to form morpholin-3-one **20**. Reduction of the amide bond led to optically pure morpholine **21**, which was used as an amino substrate in the reductive amination, Boc-deprotection sequence to form piperidine **22**. Previously described[20] aminotriazole formation was used to form the final product **OATD-01** with 15% overall yield.

The pharmacokinetic (PK) properties of **OATD-01** were evaluated based on mouse, rat, and dog single dose administrations of the compound (iv and po) under fasting conditions in the following doses: 2 mg/kg (iv), 3 mg/kg (iv), 6 mg/kg (po), 10 mg/kg (po). As formulations, aqua solutions of solutol, glucose, and/or ethanol were examined. The concentrations of **OATD-01** in animal plasma samples were monitored by LC/MS–MS analysis, until 24 h after dose (Figure 2). Mean PK parameters of individual species calculated by the noncompartmental model (NCA) are shown in Table 2.

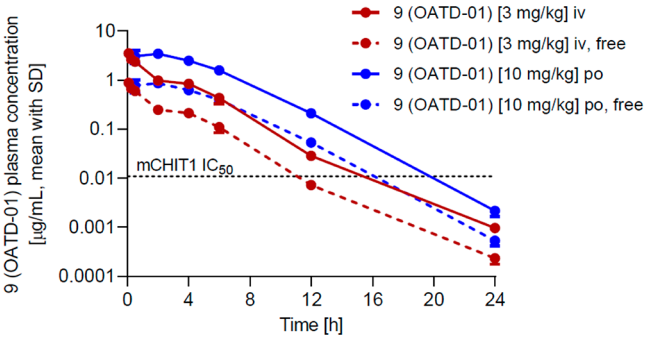

Figure 2. Plasma concentration time–course for compound **OATD-01** after single intravenous 3 mg/kg (iv) bolus and after 10 mg/kg oral administration (po) into female BALB/c mice. Free concentrations were obtained based on in vitro plasma protein binding (PPB); unbound fraction (fu) in mice is 0.253.

OATD-01 showed a favorable pharmacokinetic profile in the studied species in all formulations. Following iv dosing, **OATD-01** was characterized by low clearance (0.1–0.35 (L/h)/kg) and moderate volume of distribution (1–2 L/kg). Following po administration, systematic exposure expressed by AUC_{0-24} ranged between 5.5 and 31 mg·h/L, depending on species and formulation, while C_{max} (in the range of 2.2–7.6 mg/L) was reached in 30 min (dogs) to 2 h (rodents) after dosing. Following fast absorption, **OATD-01** was eliminated with an elimination half-life of 1.9–4.5 h in rodents and 23 h in dogs, which is comparable to intravenous administration of the compound. **OATD-01** showed high bioavailability (from 77 to 107%) in tested species and formulations.

Pharmacodynamics in Lungs. In order to evaluate the PK/PD relationship of **OATD-01** in mice, the chitinolytic activity (the pharmacodynamic marker) in plasma and lungs upon oral administration of **OATD-01** was monitored. Mice were administered with one or two doses of **OATD-01** (30 mg/kg) under fasting conditions. Plasma and perfused lungs, collected before and at defined time points up to 24 h after the last dose, were used for the determination of the levels of **OATD-01** and chitinolytic activity. As shown in Figure 3, a decrease in chitinolytic activity following **OATD-01** administration was concomitant with the increasing concentration of **OATD-01** in plasma and lung tissue, thus demonstrating target engagement *in vivo* in both plasma and lungs. Single administration of **OATD-01** resulted in at least 70% reduction of chitinolytic activity in plasma for up to 12 h. Sequential two doses of **OATD-01**, separated by 8 h led to more sustained inhibition of chitinolytic activity levels over time. Among the tested time points, the peak of compound activity was detected at 0.5 h after dosing in either scheme of administration.

In Vivo Therapeutic Efficacy of OATD-01. CHIT1 was suggested to be the main chitinase active in the human lungs[12] that facilitates pulmonary fibrotic response.[16] Further studies were carried out to evaluate direct antifibrotic effects of **OATD-01** due to additional inhibition of CHIT1 in a robust model of pulmonary interstitial fibrosis induced by administration of bleomycin. Our recent studies (data not shown) showed that CHIT1 is induced in the lungs of bleomycin

Table 2. Mean Pharmacokinetic Parameters of OATD-01 in Mice, Rats, and Dogs Determined by the Noncompartmental Model (NCA)[a]

	species					
	rat	mouse	dog	rat	mouse	dog
route	iv	iv	iv	po	po	po
sex	male	female	male	male	female	male
dose (mg/kg)	2	3	3	6	10	10
AUC_{0-24} (mg·h/L)	5.56	8.60	31.01	20.28	22.18	94.13
AUC_{0-24}/D (kg·mg·h/(L·mg))	2.78	2.87	10.34	3.38	2.22	9.41
C_0 or C_{max} (mg/L)	1.00	3.97	2.47	2.21	3.42	7.64
C_{max}/D (kg·mg/(L·mL))	n/a	n/a	0.82	0.37	0.34	0.76
T_{max} (h)	n/a	n/a	n/a	2.00	2.00	0.5*
$T_{1/2}$ (h)	4.49	2.09	21.94	4.47	1.88	22.87
CL ((L/h)/kg) (0–inf)	0.34	0.35	x	n/a	n/a	n/a
CL ((L/h)/kg) *(0–24)*	0.34	0.35	0.10	n/a	n/a	n/a
V_{ss} (L/kg) (0–24)	1.82	1.01	0.96	n/a	n/a	n/a
bioavailability (%)	n/a	n/a	n/a	107.46	77.38	91.42
formulation	A	B	C	A	B	C

[a]A, mix of ethanol and solutol (aq solution); B, mix of solutol and glucose (aq solution); C, glucose (aq solution); n/a, not applicable; x, not calculated as the % AUC extrapolated (% exp) was greater than 20%; T_{max}, calculated from analytical data; *, median.

https://dx.doi.org/10.1021/acs.jmedchem.0c01179
J. Med. Chem. XXXX, XXX, XXX–XXX

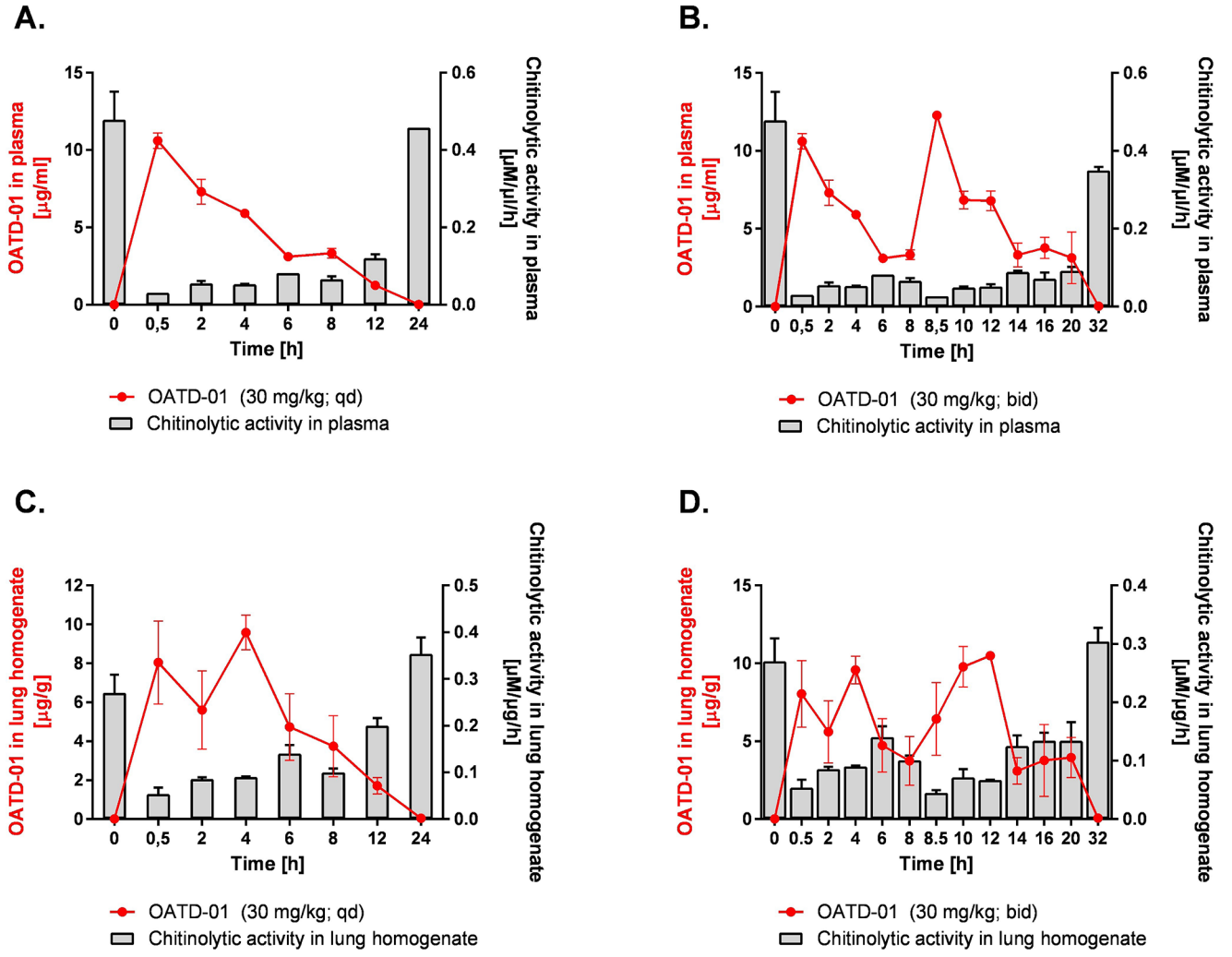

Figure 3. Relationship between total OATD-01 concentration in plasma (A, B) and lungs (C, D) following single (A, C) or double (8 h interval between doses; B, D) administration of **OATD-01** at 30 mg/kg.

administered mice; its expression is mostly restricted to macrophage population and correlated with fibrotic gene signature in the lungs. Therefore, antifibrotic efficacies of both **OATD-01** (30, 100 mg/kg, po; q.d.) and designated clinically approved therapeutic, nintedanib (100 mg/kg; po; q.d.), were evaluated using semiquantitative Ashcroft scoring scale[47,48] of the lungs of bleomycin-induced model in a therapeutic regimen (d7−d21), (Figure 4A,B). This analysis revealed that **OATD-01** significantly reduced the degree of lung fibrosis (Figure 4B) in a dose-dependent manner, ultimately achieving comparable therapeutic efficacy to reference treatment with nintedanib in this animal model. Moreover, these results correlated with a significant reduction of bleomycin-induced chitinolytic activity in plasma (Figure 4C), as opposed to nintedanib treatment confirming that CHIT1 inhibition is one of potential mechanisms to reduce fibrotic lesions in bleomycin-induced pulmonary fibrosis, and potential new strategy for IPF treatment.

CONCLUSIONS

An advanced lead molecule **3** was modified and its overall activity optimized. The strategic placement of the "magic methyl" group significantly changed its in vitro activity profile and led to the identification of the molecule **OATD-01**. **OATD-01** is a highly potent CHIT1 inhibitor, also inhibiting AMCase, with excellent PK properties across multiple animal species. Given once daily in a range of doses between 30 and 100 mg/kg orally in vivo, it showed significant antifibrotic efficacy in preclinical animal model of bleomycin-induced pulmonary fibrosis in mice. Provided data package for **OATD-01** and its antifibrotic efficacy in preclinical models in vivo will hopefully lay the grounds for novel therapeutic approach in IPF and possibly other fibrosis-related clinical indications such as NASH. The preclinical studies have shown that the **OATD-01** is well tolerated, has low toxicity, and has a favorable pharmacokinetic profile. **OATD-01** is currently being clinically studied (completed phase 1b).

EXPERIMENTAL SECTION

Chemical Methods. All solvents, substrates, and reagents that were commercially available were used without further purification. TLC analysis was performed using precoated glass plates (0.2 ± 0.03 mm thickness, GF-254, particle size 0.01−0.04 mm) from Fluorochem Ltd., U.K. Column chromatography was performed using high-purity grade silica gel (pore size 60 Å, 220−440 mesh particle size, 35−75 μm particle size) from Fluka. Preparative HPLC was performed on LC-20AP Shimadzu with ELSD-LTII detector equipped with Hypersil GOLD 21.2/250 mm, 5 μm C18 column. ^{1}H NMR spectra were recorded on Agilent Mercury 400 MHz

https://dx.doi.org/10.1021/acs.jmedchem.0c01179
J. Med. Chem. XXXX, XXX, XXX−XXX

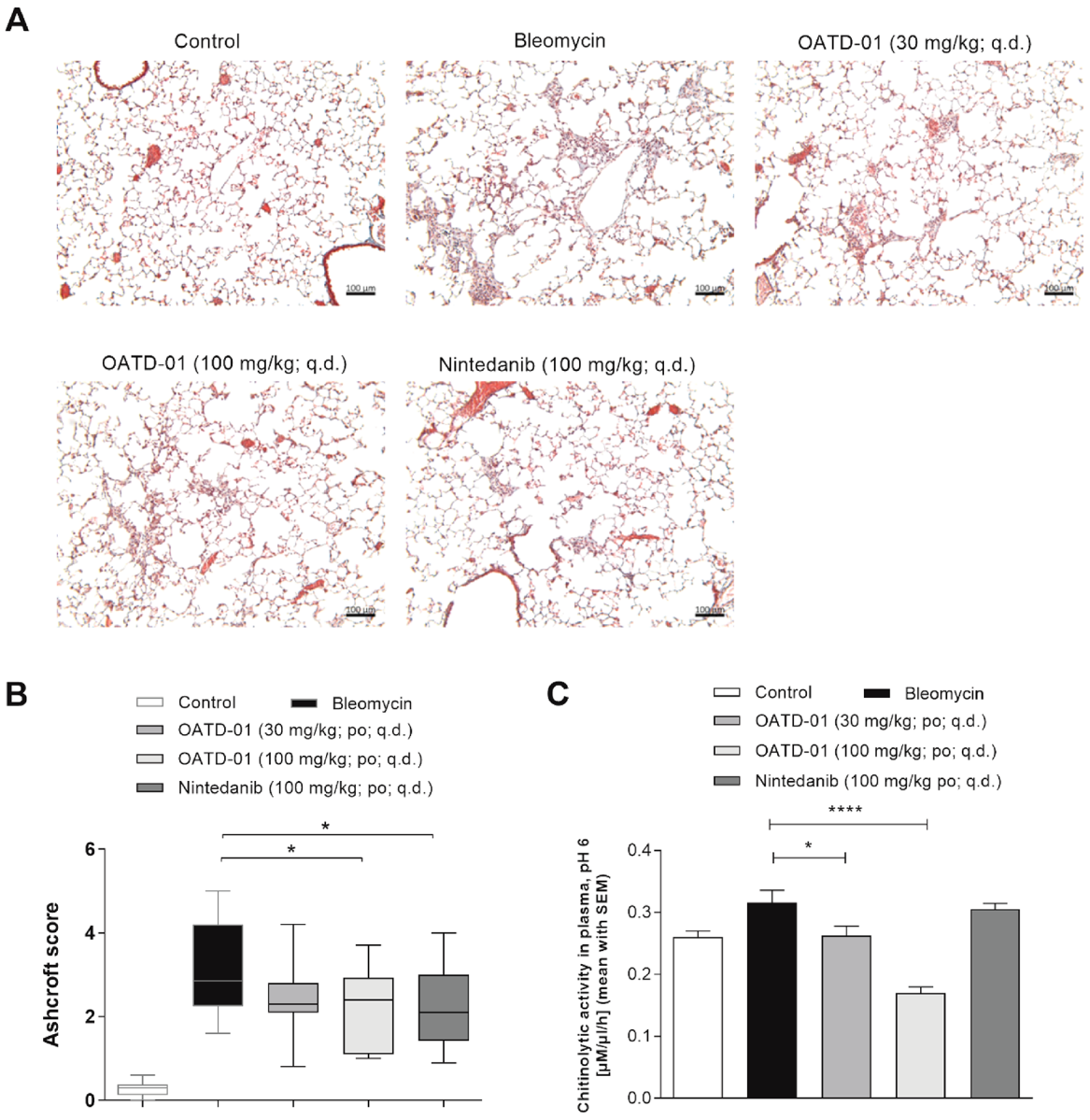

Figure 4. OATD-01 treatment ameliorates bleomycin-induced lung fibrosis in a dose-dependent manner. (A) Representative Masson's trichrome staining of pulmonary fibrosis 21 days after bleomycin injury, with or without treatment with **OATD-01** or nintedanib. (B) Semiquantitative analysis of pulmonary fibrosis by Ashcroft score (0−6) in the lung sections (n = 3 per animal) with or without **OATD-01** (30 and 100 mg/kg; q.d.) and nintedanib (100 mg/kg; q.d.) as compared to vehicle treated controls. (C) Chitinolytic activity in plasma collected 24 h after the last dose of **OATD-01** (30 and 100 mg/kg; q.d.) or nintedanib (100 mg/kg; q.d.) as compared to vehicle treated controls. Data are presented as the mean ± SEM. P-values of <0.05 were considered as statistically significant and presented as ∗ for $p < 0.05$, ∗∗ for $p < 0.01$, ∗∗∗ for $p < 0.001$, and ∗∗∗∗ for $p < 0.0001$.

spectrometer and on Bruker AVANCE DRX500, AVANCE DRX600, or Bruker AVANCE II PLUS (respectively at 500, 600, or 700 MHz) NMR spectrometers. All spectra were recorded in appropriate deuterated solvents ($CDCl_3$, DMSO-d_6, D_2O, methanol-d_4, etc.) that were commercially available. Resonances are given in parts per million relative to tetramethylsilane. Data are reported as follows: chemical shift, multiplicity (s = singlet, d = doublet, t = triplet, m = multiplet, br = broad), coupling constants (J in Hz), and integration. LC−MS spectra were recorded on a Shimadzu LC-20AD LPG separation module with a SPD-M20A UV detector and LCMS-2020 mass detector equipped with Kinetex 2.1/50 mm, 2.6 μm C18 column eluted with 0.5 mL/min flow of 10−90% gradient (over 6 min) of acetonitrile in water. Purities of all final reported compounds were greater than 95% based on HPLC chromatograms. Purification of the final compounds by preparative HPLC was accomplished on C-18 250 mm × 21 mm column in 0.05% TFA in water/acetonitrile 95:5 → 45:55 gradient over 30 min followed by freeze-drying of the pooled fractions containing pure products. In some cases, the so obtained trifluoroacetate salts of the final compounds were judged to be of insufficient quality for biological testing due to their physical appearance (oils with a distinguished scent of trifluoroacetic acid). Therefore, they were redissolved in a small amount of 0.1 M HCl and subjected to the second lyophilization providing well-behaving hydrochloride salts.

Synthesis of compounds **5**, **7**, **8**, and **15**−**17** are described in Supporting Information.

(*S*)-4-(1-(5-Amino-4*H*-1,2,4-triazol-3-yl)piperidin-4-yl)-3-(4-chlorobenzyl)thiomorpholine 1,1-Dioxide (5). ^{1}H NMR (500 MHz, DMSO-d_6) δ 7.31 (m, $J_{AA'BB'}$ = 8.5 Hz, 2H), 7.24 ($J_{AA'BB'}$ = 8.5 Hz, 2H), 5.48 (bs, 2H), 3.71−3.64 (m, 2H), 3.52−3.43 (m, 1H), 3.11−2.96 (m, 3H), 2.94−2.79 (m, 4H), 2.78−2.70 (m, 1H), 2.64−2.52 (m, 2H), 1.65−1.55 (m, 2H), 1.37−1.18 (m, 3H); ^{1}H NMR

https://dx.doi.org/10.1021/acs.jmedchem.0c01179
J. Med. Chem. XXXX, XXX, XXX−XXX

(700 MHz, DMSO-d_6 + D_2O, 348 K) δ 7.32−7.29 (m, 2H), 7.29−7.20 (m, 2H), 3.79−3.63 (m, 2H), 3.63−3.52 (m, 1H), 3.40−3.31 (m, 1H), 3.19−3.12 (m, 1H), 3.06−2.99 (m, 2H), 2.99−2.76 (m, 5H), 2.72−2.60 (m, 2H), 1.69−1.61 (m, 2H), 1.45−1.25 (m, 2H); ^{13}C NMR (176 MHz, DMSO-d_6) δ 138.3, 131.7 (2×), 131.3, 128.7 (2×), 60.4, 57.5, 55.8, 52.2, 50.2, 46.0, 45.9, 41.5, 35.2, 30.2, 28.0, 21.2; HRMS (ESI) m/z calcd for $C_{18}H_{26}ClN_6O_2S$ $[M + H]^+$ 425.1521 found 425.1533.

(*S*)-5-(4-(2-(4-Chlorobenzyl)-4-methylpiperazin-1-yl)-piperidin-1-yl)-4*H*-1,2,4-triazol-3-amine (6).[38] ^{1}H NMR (500 MHz, DMSO-d_6) δ 10.86 (bs, 1H), 7.32−7.26 (m, 2H), 7.17 (d, J = 8.0 Hz, 2H), 5.59 (s, 2H), 3.77−3.67 (m, 2H) 2.91−2.71 (m, 3H), 2.70−2.51 (m, 7H), 2.00 (s, 3H), 1.98−1.90 (m, 2H),1.75−1.55 (m, 2H), 1.49−1.22 (m, 2H); ^{1}H NMR (700 MHz, DMSO-d_6) δ 7.42−7.28 (m, 2H), 7.28−7.15 (m, 2H), 3.88−3.65 (m, 2H), 2.97−2.88 (m, 1H), 2.88−2.79 (m, 2H), 2.76−2.62 (m, 3H), 2.62−2.53 (m, 2H), 2.38−2.23 (m, 2H), 2.11−1.99 (m, 5H), 1.78−1.73 (m, 1H), 1.69−1.64 (m, 1H), 1.53−1.46 (m, 1H), 1.41−1.30 (m, 1H); ^{13}C NMR (176 MHz, DMSO-d_6) δ 139.7, 131.5 (2×), 130.8, 128.6 (2×), 58.8, 56.7, 55.74, 55.66, 46.5, 46.3, 46.1, 43.7, 40.5, 32.7, 30.1, 25.9 (one signal is missing due to overlap); HRMS (ESI) m/z calcd for $C_{19}H_{29}ClN_7$ $[M + H]^+$ 390.2167 found 390.2173.

(*S*)-4-(1-(5-Amino-4*H*-1,2,4-triazol-3-yl)piperidin-4-yl)-3-(4-chlorobenzyl)piperazin-2-one 2,2,2-Trifluoroacetate (7). ^{1}H NMR (500 MHz, DMSO-d_6) δ 7.88 (s, 1H), 7.32−7.22 (m, 4H), 3.85−3.59 (m, 4H), 3.15−2.75 (m, 8H), 1.73 (d, J = 12.2 Hz, 1H), 1.66−1.53 (m, 1H), 1.51−1.28 (m, 2H); ^{1}H NMR (700 MHz, DMSO-d_6 + D_2O, 348 K) δ 7.34−7.20 (m, 4H), 3.73−3.55 (m, 3H), 3.24−3.17 (m, 1H), 3.11−3.01 (m, 3H), 2.99−2.76 (m, 5H), 1.75−1.62 (m, 2H), 1.51−1.33 (m, 2H); ^{13}C NMR (176 MHz, DMSO-d_6) δ 159.4, 137.4, 131.9 (2×), 131.5, 128.3 (2×), 62.0, 57.2, 45.7, 45.6, 41.3, 40.0, 38.5, 35.1, 28.3, 27.0, 25.2; HRMS (ESI) m/z calcd for $C_{18}H_{25}ClN_7O$ $[M + H]^+$ 390.1804 found 390.1809.

(*S*)-4-(1-(5-Amino-4*H*-1,2,4-triazol-3-yl)piperidin-4-yl)-5-(4-chlorobenzyl)piperazin-2-one 2,2,2-Trifluoroacetate (8). ^{1}H NMR (500 MHz, D_2O) δ 7.28 ($J_{AA'BB'}$ = 7.3 Hz, 2H), 7.14 ($J_{AA'BB'}$ = 7.7 Hz, 2H), 4.07−4.12 (m, 1H), 4.01 (d, J = 16.7 Hz, 1H), 3.86 (d, J = 16.9 Hz, 1H), 3.73−3.77 (m, 2H), 3.32−3.36 (m, 1H), 3.17−3.22 (m, 2H), 2.81−3.04 (m, 4H), 2.09−2.15 (m, 2H), 1.68−1.75 (m, 2H); ^{1}H NMR (700 MHz, DMSO-d_6 + D_2O, 348 K) δ 7.41−7.24 (m, 4H), 3.87−3.77 (m, 2H), 3.74−3.69 (m, 1H), 3.67−3.62 (m, 1H), 3.60−3.52 (m, 1H), 3.37−3.23 (m, 3H), 3.12−3.07 (m, 1H), 3.06−2.99 (m, 1H), 2.99−2.86 (m, 2H), 2.82−2.72 (m, 1H), 2.02−1.91 (m, 2H), 1.71−1.56 (m, 2H); ^{13}C NMR (176 MHz, DMSO-d_6) δ 159.2, 135.0, 132.4, 131.7 (2×), 129.2 (2×), 59.2, 54.3, 48.1, 47.4, 45.3, 45.1, 40.3, 40.0, 26.4, 25.4, 24.5; HRMS (ESI) m/z calcd for $C_{18}H_{25}ClN_7O$ $[M + H]^+$ 390.1804 found 390.1821.

5-(4-((2*S*,5*S*)-5-(4-Chlorobenzyl)-2-methylmorpholino)-piperidin-1-yl)-4*H*-1,2,4-triazol-3-amine Hydrochloride (9).

*Step 1. Synthesis of (S)-2-Amino-3-(4-chlorophenyl)propan-1-ol (**18**).* To a solution of 4-chloro-L-phenylalanine (20.0 g; 100 mmol) in tetrahydrofuran (200 mL) borane dimethylsulfide complex (28.16 mL; 300 mmol) was added dropwise at 0 °C (foaming!). After addition was complete, the cooling bath was removed, and the reaction mixture was refluxed for 5 h. The reaction progress was monitored by LC−MS. The reaction mixture was cooled to room temperature and 6 N HCl aq (100 mL) was carefully added (foaming!) and then refluxed for an additional 1 h. The reaction mixture was cooled to room temperature, 4 N NaOH aq was added to reach pH 12 and subsequently extracted with ethyl acetate (2 × 500 mL). The combined organic layers were dried over anhydrous $MgSO_4$, filtered, and concentrated in vacuo. The oily residue was triturated with diethyl ether and the solids were filtered off to give (*S*)-2-amino-3-(4-chlorophenyl)propan-1-ol (**18**) as a white solid in 89% yield (16.5 g; 88.88 mmol). ESI-MS m/z for $C_9H_{12}ClNO$ found 185.7/187.7 $[M + H]^+$; ^{1}H NMR (500 MHz, $CDCl_3$) δ 7.28 (d, J = 8.3 Hz, 2H), 7.11 (d, J = 8.3 Hz, 2H), 3.62 (dd, J = 10.6, 3.8 Hz, 1H), 3.37 (dd, J = 10.5, 6.9 Hz, 1H), 3.11−3.07 (brs, 1H), 2.76 (dd, J = 13.6, 5.4 Hz, 1H), 2.50 (dd, J = 13.6, 8.6 Hz, 1H).

*Step 2. Synthesis of (R)-2-Bromo-N-((S)-1-(4-chlorophenyl)-3-hydroxypropan-2-yl)propanamide (**19**).* To the solution of alcohol **18** (1 g; 4.5 mmol) and (*R*)-2-bromopropionic acid (0.4 mL; 4.5 mmol) in DCM (30 mL) at 0 °C, diisopropylethylamine (DIPEA; 2.35 mL; 13.5 mmol) and TBTU (1.44 g; 4.5 mmol) were added sequentially, and the reaction mixture was stirred at this temperature for 3 h. After this time TLC control showed complete consumption of the starting materials, so the reaction mixture was transferred to the separatory funnel and washed sequentially with 1 M HCl, 1 M K_2CO_3. The organic phase was dried over anhydrous $MgSO_4$, filtered, and concentrated in vacuo, and the crude product was purified by flash column chromatography (DCM/MeOH 100:1 v/v), and product **19** was obtained as a white solid in 64% yield (0.6 g; 2.88 mmol). ESI-MS m/z for $C_{12}H_{16}BrClNO_2$ found 320.7/322.7 $[M + H]^+$; ^{1}H NMR (500 MHz, $CDCl_3$) δ 7.25 (d, J = 8.2 Hz, 2H), 7.14 (d, J = 8.2 Hz, 2H), 6.58 (d, J = 6.7 Hz, 1H), 4.33 (dd, J = 14.1, 7.1 Hz, 1H), 4.13−4.06 (m, 1H), 3.69−3.64 (m, 1H), 3.61−3.57 (m, 1H), 2.90−2.81 (m, 2H), 2.17 (brs, 1H), 1.82 (d, J = 6.9 Hz, 3H).

*Step 3. Synthesis of (2S,5S)-5-(4-Chlorobenzyl)-2-methylmorpholin-3-one (**20**).* To the solution of compound **19** (1.46 g; 4.52 mmol) in THF (45 mL) sodium hydride (NaH) (60% in mineral oil; 0.65 g; 13.56 mmol) was added in one portion and stirred at room temperature for 30 min. TLC showed consumption of the starting material. The reaction was quenched by addition of water and then extracted with diethyl ether. Combined organic extracts were then washed with brine, dried over anhydrous $MgSO_4$, filtered, and concentrated in vacuo to provide product **20** as a white solid after washing with hexane in 77% yield (0.83 g; 3.46 mmol). ESI-MS m/z for $C_{12}H_{15}ClNO_2$ found 240.1/242.1 $[M + H]^+$; ^{1}H NMR (500 MHz, $CDCl_3$) δ 7.27 (d, J = 8.2 Hz, 2H), 7.10 (d, J = 8.2 Hz, 2H), 6.13 (brs, 1H), 4.18 (m, 1H), 3.76 (d, J = 3.0 Hz, 2H), 3.55−3.50 (m, 1H), 2.91−2.83 (m, 2H), 1.46 (d, J = 6.9 Hz, 3H).

*Step 4. Synthesis of (2S,5S)-5-(4-Chlorobenzyl)-2-methylmorpholine (**21**).* To the solution of lactam **20** (1.03 g; 4.29 mmol) in tetrahydrofuran (21.25 mL) borane dimethylsulfide complex (1.2 mL; 12.89 mmol) was added dropwise at 0 °C (foaming!). The cooling bath was removed, and the reaction mixture was refluxed for 2 h. LC−MS analysis showed consumption of the starting material. The mixture was cooled to room temperature, and 6 M HCl aq (10 mL) was carefully added (foaming!), then refluxed for another 1 h. The reaction mixture was cooled to room temperature and 4 M NaOH aq was added to reach pH 10 and then extracted with ethyl acetate (2 × 50 mL). The combined organic phases were dried over $MgSO_4$, filtered, and concentrated in vacuum to give product **21** as a colorless oil in 90% yield (871 mg; 3.86 mmol). ESI-MS m/z for $C_{12}H_{17}ClNO$ found 226.4/228.4 $[M + H]^+$; ^{1}H NMR (500 MHz, DMSO-d_6 + D_2O) δ 7.33 (d, J = 8.3 Hz, 2H), 7.23 (d, J = 8.3 Hz, 2H), 3.50−3.48 (m, 1H), 3.49−3.47 (m, 2H), 2.87−2.81 (m, 1H), 2.80−2.76 (m, 2H), 2.65 (dd, J = 12.4 Hz, 8.3 Hz, 1H), 2.58 (dd, J = 12.4 Hz, 3.0 Hz, 1H), 1.09 (d, J = 6.2 Hz, 3H).

*Step 5. Synthesis of (2S,5S)-5-(4-Chlorobenzyl)-2-methyl-4-(piperidin-4-yl)morpholine Hydrochloride (**22**).* To a solution of compound **21** (1.36 g; 6.02 mmol) in 1,2-dichloroethane (4 mL) Boc-piperidone (1.8 g; 9.03 mmol) was added followed by acetic acid (0.69 mL; 12.4 mmol), and the reaction mixture was stirred for 4 h at ambient temperature. Sodium triacetoxyborohydride $[NaBH(OAc)_3]$ (2.61 g; 12.4 mmol) was then added in one portion, and the reaction mixture was stirred overnight at ambient temperature. To this mixture 5% aq $NaHCO_3$ (10 mL) was added, and after stirring for 5 min the mixture was extracted with dichloromethane (2 × 20 mL). The organic phases were combined, dried over anhydrous $MgSO_4$, filtered, and concentrated in vacuum. The residue was purified by flash chromatography (DCM/MeOH 100:0 to 200:1 v/v) white foam (1.10 g; 2.68 mmol; 45% yield) was treated with 3M HCl(g)/AcOEt (26.8 mL), and the reaction mixture was stirred for 40 min at ambient temperature. The solvent was removed in vacuo and residue was triturated with diethyl ether and filtered to give product **22** as a hydrochloride salt as a white solid in 34% yield (640 mg; 1.85 mmol). ESI-MS m/z for $C_{17}H_{26}ClN_2O$ found 309.9/311.9 $[M + H]^+$; ^{1}H NMR (500 MHz, DMSO-d_6) δ 7.35 (d, J = 8.4 Hz, 2H), 7.33 (d, J =

https://dx.doi.org/10.1021/acs.jmedchem.0c01179
J. Med. Chem. XXXX, XXX, XXX−XXX

8.4 Hz, 2H), 4.04 (brs, 2H), 3.59 (brs, 2H), 3.45 (brs, 1H), 3.40 (m, 1H), 3.39−3.36 (m, 2H), 3.10 (brs, 2H), 2.98 (brs, 1H), 2.87 (brs, 2H), 2.31 (brs, 2H), 2.17 (brs, 2H), 1.21 (d, J = 6.2 Hz, 3H).

*Step 6. Synthesis of 5-(4-((2S,5S)-5-(4-Chlorobenzyl)-2-methylmorpholino)piperidin-1-yl)-4H-1,2,4-triazol-3-amine Hydrochloride (**9**).* To a solution of piperidine **22** (640 mg; 1.85 mmol) in acetonitrile (10.0 mL) was added *S*,*S*-dimethyl *N*-cyanodithioiminocarbonate (298 mg; 2.03 mmol) followed by potassium carbonate (563 mg; 4.07 mmol), and the reaction mixture was refluxed for 1.5 h. LC−MS analysis showed consumption of the starting material. To this mixture hydrazine monohydrate (0.27 mL; 5.55 mmol) was added, and reflux was maintained for an additional 2 h. The reaction mixture was cooled down to ambient temperature, filtered, and the filtrate was concentrated in vacuo. The residue was purified by flash chromatography (DCM/MeOH 250:1 to 50:1 v/v). The material obtained after evaporation of solvents was dissolved in a small amount of AcOEt, and then 3 M HCl/AcOEt (20 mL) was added. The mixture was stirred for 5 min and concentrated in vacuo. The residue was dissolved in methanol (2 mL) and as a solution was added dropwise to vigorously stirred diethyl ether (250 mL). Stirring was continued for an additional 20 min at room temperature and then the precipitate was filtered off to give product **9** as a hydrochloride salt as a white solid in 72% yield (568 mg; 1.33 mmol). ^{1}H NMR (500 MHz, DMSO-d_6) δ 7.39 (d, J = 8.3 Hz, 2H), 7.30 (d, J = 8.3 Hz, 2H), 3.87−3.79 (m, 3H), 3.66 (brs, 2H), 3.58 (brs, 1H), 3.52−3.45 (m, 2H), 3.09 (brs, 2H), 3.00−2.93 (m, 2H), 2.92−2.88 (m, 1H), 2.20 (brs, 2H), 1.67 (brs, 2H), 1.20 (d, J = 6.2 Hz, 3H); ^{1}H NMR (700 MHz, C_6D_6/methanol-d_4) δ 7.13 (d, J = 8.2 Hz, 2H), 6.89 (d, J = 8.2 Hz, 2H), 3.99 (br s, 2H), 3.66 (br s, 3H), 3.56 (d, J = 11.4 Hz, 1H), 3.54−3.46 (m, 1H), 3.37 (d, J = 11.4 Hz, 1H), 2.90−2.80 (m, 3H), 2.68 (d, J = 10.4 Hz, 1H), 2.40 (d, J = 11.9 Hz, 2H), 2.32−2.25 (m, 1H), 2.05 (t, J = 11.2 Hz, 1H), 1.81 (d, J = 12.5 Hz, 1H), 1.65 (d, J = 12.5 Hz, 1H), 1.54−1.46 (m, 1H), 1.46−1.37 (m, 1H) and 1.11 (d, J = 6.2 Hz, 3H); ^{1}H NMR for free base (400 MHz, methanol-d_4) δ 7.32−7.23 (m, 2H), 7.21−7.12 (m, 2H), 3.88−3.77 (m, 2H), 3.66−3.52 (m, 2H), 3.51−3.42 (m, 1H), 3.02−2.92 (m, 2H), 2.91−2.76 (m, 4H), 2.72−2.63 (m, 1H), 2.43−2.30 (m, 1H), 2.09−1.98 (m, 2H), 1.56−1.37 (m, 2H), 1.18 (d, J = 6.2 Hz, 3H); ^{13}C NMR (175 MHz, C_6D_6) δ 139.0, 132.1, 131.2, 129.0, 128.1, 72.6, 67.8, 56.5, 55.7, 50.1, 48.9, 45.8, 45.7, 29.7, 29.2, 27.7, 19.3; ^{13}C NMR for free base (101 MHz, methanol-d_4) δ 138.7, 131.5, 130.6 (2×), 128.2 (2×), 72.3, 67.1, 56.2, 55.3, 49.5, 45.26, 45.25, 29.0, 28.5, 26.7, 18.0 (two signals are missing due to overlap); HRMS (ESI) m/z calcd for $C_{19}H_{28}ClN_6O$ $[M + H]^+$ 391.2008 found 391.2004.

5-(4-((2*R*,5*S*)-5-(4-Chlorobenzyl)-2-methylmorpholino)-piperidin-1-yl)-4*H*-1,2,4-triazol-3-amine Hydrochloride (10). The title compound **10** was obtained as a hydrochloride salt (3% overall yield) in the same manner as molecule **9** with the exception that (2*S*)-2-bromopropionic acid instead of (2*R*)-2-bromopropionic acid was used in the second synthetic step. ^{1}H NMR (700 MHz, DMSO-d_6) δ 7.41 (d, J = 8.4 Hz, 2H), 7.35 (d, J = 8.4 Hz, 2H), 4.08 (br s, 1H), 3.91−3.84 (m, 2H), 3.83−3.80 (m, 2H), 3.70−3.67 (m, 2H), 3.48 (d, J = 12.7 Hz, 2H), 2.87 (t, J = 11.6 Hz, 1H), 2.75 (t, J = 11.5 Hz, 1H), 2.70 (dd, J = 14.5, 7.7 Hz, 1H), 2.65 (t, J = 12.0 Hz, 1H), 1.80−1.90 (m, 2H), 1.63 (qd, J = 12.3, 4.2 Hz, 1H), 1.11 (d, J = 6.2 Hz, 3H); ^{13}C NMR (176 MHz, DMSO-d_6) δ 135.7, 132.1, 131.4 (2×), 129.2 (2×), 69.5, 67.3, 58.7, 57.8, 50.3, 45.6, 45.3, 40.5, 31.7, 26.2, 22.5, 18.6 (one signal is missed due to overlap); HRMS (ESI) m/z calcd for $C_{19}H_{28}ClN_6O$ $[M + H]^+$ 391.2008 found 391.2015.

5-(4-((2*S*,5*S*)-5-(4-Chlorobenzyl)-2-ethylmorpholino)-piperidin-1-yl)-4*H*-1,2,4-triazol-3-amine Hydrochloride (11). The title compound **11** was obtained as a hydrochloride salt (7% overall yield) in the same manner as molecule **9** with the exception that (2*R*)-2-bromobutanoic acid instead of (2*R*)-2-bromopropionic acid was used in the second synthetic step. ^{1}H NMR (500 MHz, DMSO-d_6 + D_2O) δ 7.38 (d, $J_{AA'BB'}$ = 8.5 Hz, 2H), 7.27 (d, $J_{AA'BB'}$ = 8.3 Hz, 2H), 3.81 (brd, J = 12.8 Hz, 2H), 3.67−3.69 (m, 1H), 3.52−3.56 (m, 4H), 3.38−3.41 (m, 1H), 2.99−3.06 (m, 3H), 2.85−2.93 (m, 2H), 2.15−2.21 (m, 2H), 1.48−1.60 (m, 4H), 0.89 (t, J = 7.5 Hz, 3H); ^{1}H NMR (700 MHz, DMSO-d_6 + D_2O, 348 K) δ 7.41−7.36 (m, 2H), 7.36−7.29 (m, 2H), 3.94−3.85 (m, 2H), 3.80−3.77 (m, 1H), 3.74−3.68 (m, 2H), 3.67−3.46 (m, 3H), 3.16−3.10 (m, 2H), 3.10−3.01 (m, 1H), 3.01−2.90 (m, 2H), 2.28−2.12 (m, 2H), 1.83−1.72 (m, 2H), 1.64−1.48 (m, 2H), 0.95 (t, J = 7.5 Hz, 3H); ^{13}C NMR (176 MHz, DMSO-d_6) δ 135.0, 132.3, 132.0 (2×), 129.2 (2×), 75.1, 64.9, 58.7, 55.5, 51.9, 47.3, 45.3, 45.1, 40.0, 38.9, 27.3, 25.8, 25.7, 9.5; HRMS (ESI) m/z calcd for $C_{20}H_{30}ClN_6O$ $[M + H]^+$ 405.2164 found 405.2166.

5-(4-((2*S*,5*S*)-5-(4-Chlorobenzyl)-2-isopropylmorpholino)-piperidin-1-yl)-4*H*-1,2,4-triazol-3-amine 2,2,2-Trifluoroacetate (12). The title compound **12** was obtained as a TFA salt (2% overall yield) in the same manner as example **9** with the exception that (2*R*)-2-bromo-3-methylbutanoic acid instead of (2*R*)-2-bromopropionic acid was used in the second synthetic step. ^{1}H NMR (700 MHz, DMSO-d_6) δ 10.15 (s, 1H), 7.45−7.41 (m, 2H), 7.36−7.31 (m, 2H), 7.05 (bs, 2H), 3.88 (t, J = 16.8 Hz, 2H), 3.83−3.75 (m, 1H), 3.63−3.53 (m, 3H), 3.49−3.37 (m, 2H), 3.17−3.07 (m, 1H), 3.03 (t, J = 12.5 Hz, 1H), 2.94 (t, J = 12.8 Hz, 1H), 2.84 (t, J = 12.5 Hz, 1H), 2.28 (d, J = 12.0 Hz, 1H), 2.22 (d, J = 12.2 Hz, 1H), 1.82 (ddd, J = 13.7, 9.4, 5.9 Hz, 1H), 1.69−1.59 (m, 2H), 0.97 (d, J = 6.9 Hz, 3H), 0.96 (d, J = 6.9 Hz, 3H); ^{13}C NMR (176 MHz, DMSO-d_6) δ 134.9, 132.4, 131.9 (2×), 129.2 (2×), 78.2, 64.9, 61.3, 58.8, 55.5, 45.8, 45.3, 45.1, 39.9, 30.7, 27.3, 25.8, 25.6, 18.6, 17.3; HRMS (ESI) m/z calcd for $C_{21}H_{32}ClN_6O$ $[M + H]^+$ 419.2321 found 419.2325.

5-(4-((2*S*,5*S*)-5-(4-Chlorobenzyl)-2-isobutylmorpholino)-piperidin-1-yl)-4*H*-1,2,4-triazol-3-amine 2,2,2-Trifluoroacetate (13). The title compound **13** was obtained as a TFA salt (3% overall yield) in the same manner as example **9** with the exception that (2*R*)-2-bromo-4-methylpentanoic acid instead of (2*R*)-2-bromopropionic acid was used in the second synthetic step. ^{1}H NMR (700 MHz, DMSO-d_6) δ 7.43 (d, J = 8.4 Hz, 2H), 7.34 (d, J = 8.4 Hz, 2H), 6.99 (br s, 1H), 3.89−3.85 (m, 3H), 3.79−3.47 (m, 7H), 3.12 (d, J = 7 Hz, 2H), 3.00 (s, 1H), 2.95−2.91 (m, 1H), 2.86−2.83 (m, 1H), 2.23−2.18 (m, 2H), 1.82−1.76 (m, 1H), 1.64−1.59 (m, 2H), 1.53−1.49 (m, 1H), 1.31−1.27 (m, 1H), 0.91−0.87 (m, 6H); ^{13}C NMR (176 MHz, DMSO-d_6) δ 135.0, 132.3, 131.9 (2×), 129.2 (2×), 72.6, 65.1, 60.0, 58.7, 55.6, 47.8, 45.3, 45.1, 41.3, 40.0, 27.3, 25.9, 25.6, 23.9, 23.5, 22.1; HRMS (ESI) m/z calcd for $C_{22}H_{34}ClN_6O$ $[M + H]^+$ 433.2477 found 433.2489.

((2*R*,5*S*)-4-(1-(5-Amino-4*H*-1,2,4-triazol-3-yl)piperidin-4-yl)-5-(4-chlorobenzyl)morpholin-2-yl)methanol Hydrochloride (14). The title compound **14** was obtained as a hydrochloride salt (8% overall yield) in the same manner as example **9** with the exception that (2*R*)-2-bromo-3-*tert*-butoxypropanoic acid instead of (2*R*)-2-bromopropionic acid was used in the second synthetic step. ^{1}H NMR (700 MHz, DMSO-d_6 + D_2O) δ 7.43−7.37 (m, 2H), 7.37−7.29 (m, 2H), 3.96−3.80 (m, 4H), 3.77−3.65 (m, 2H), 3.65−3.52 (m, 4H), 3.21−3.07 (m, 3H), 3.04−2.95 (m, 2H), 2.29−2.18 (m, 2H), 1.87−1.74 (m, 2H); ^{13}C NMR (176 MHz, DMSO-d_6) δ 135.0, 132.3, 132.0 (2×), 129.2 (2×), 74.7, 64.6, 61.7, 58.7, 55.5, 45.2, 45.1, 44.9, 39.9, 27.1, 25.8, 25.6 (one signal is missing due to overlap); HRMS (ESI) m/z calcd for $C_{19}H_{28}ClN_6O_2$ $[M + H]^+$ 407.1957 found 407.1969.

2-((2*R*,5*S*)-4-(1-(5-Amino-4*H*-1,2,4-triazol-3-yl)piperidin-4-yl)-5-(4-chlorobenzyl)morpholin-2-yl)propan-2-ol 2,2,2-Trifluoroacetate (15). ^{1}H NMR (600 MHz, DMSO-d_6 + D_2O) δ 7.39 ($J_{AA'BB'}$ = 8.5 Hz, 2H), 7.31 ($J_{AA'BB'}$ = 8.5 Hz, 2H), 3.89−3.77 (m, 2H), 3.75−3.69 (m, 1H), 3.67−3.53 (m, 3H), 3.46−3.37 (m, 2H), 3.21−2.97 (m, 3H), 2.97−2.86 (m, 2H), 2.25−2.16 (m, 2H), 1.64−1.55 (m, 2H), 1.15 (s, 3H), 1.14 (s, 3H); ^{1}H NMR (700 MHz, DMSO-d_6 + D_2O, 348 K) δ 7.45−7.35 (m, 2H), 7.35−7.26 (m, 2H), 3.96−3.84 (m, 2H), 3.76−3.62 (m, 4H), 3.54−3.50 (m, 2H), 3.22−3.16 (m, 1H), 3.12−3.06 (m, 2H), 2.97−2.87 (m, 2H), 2.30−2.13 (m, 2H), 1.73−1.61 (m, 2H), 1.19 (s, 6H); ^{13}C NMR (176 MHz, DMSO-d_6) δ 134.9, 132.4, 132.0 (2×), 129.2 (2×), 70.4, 65.0, 59.4, 59.01, 57.7, 55.4, 52.1, 45.3, 45.2, 44.0, 40.0, 27.2, 27.1, 25.6, 24.6; HRMS (ESI) m/z calcd for $C_{21}H_{32}ClN_6O_2$ $[M + H]^+$ 435.2270 found 435.2282.

5-(4-((2*R*,5*S*)-5-(4-Chlorobenzyl)-2-(methoxymethyl)-morpholino)piperidin-1-yl)-4*H*-1,2,4-triazol-3-amine 2,2,2-Trifluoroacetate (16). ^{1}H NMR (500 MHz, DMSO-d_6) δ 7.42 ($J_{AA'BB'}$

https://dx.doi.org/10.1021/acs.jmedchem.0c01179
J. Med. Chem. XXXX, XXX, XXX−XXX

= 8.3 Hz, 2H), 7.33 ($J_{AA'BB'}$ = 8.2 Hz, 2H), 3.91−3.80 (m, 4H), 3.64−3.53 (m, 3H), 3.53−3.44 (m, 3H), 3.30 (s, 3H), 3.15−3.02 (m, 3H), 2.94−2.86 (m, 1H), 2.85−2.79 (m, 1H), 2.21−2.12 (m, 2H), 1.66−1.55 (m, 2H); ^{1}H NMR (700 MHz, DMSO-d_6 + D_2O, 348 K) δ 7.40−7.35 (m, 2H), 7.35−7.26 (m, 2H), 3.92−3.83 (m, 3H), 3.74−3.66 (m, 2H), 3.66−3.60 (m, 2H), 3.55−3.50 (m, 2H), 3.44−3.38 (m, 1H), 3.36−3.28 (m, 3H), 3.20−3.07 (m, 3H), 2.96−2.85 (m, 2H), 2.21−2.09 (m, 2H), 1.69−1.57 (m, 2H); ^{13}C NMR (176 MHz, DMSO-d_6) δ 134.9, 132.4, 131.9 (2×), 129.2 (2×), 72.2, 64.9, 59.2, 58.84, 58.76, 55.6, 45.2, 45.1, 39.9, 27.4, 25.91, 25.89, 25.6 (one signal is missing due to overlap); HRMS (ESI) m/z calcd for $C_{20}H_{30}ClN_6O_2$ $[M + H]^+$ 421.2113 found 421.2131.

(2*R*,5*S*)-4-(1-(5-Amino-4*H*-1,2,4-triazol-3-yl)piperidin-4-yl)-5-(4-chlorobenzyl)-*N*-methylmorpholine-2-carboxamide 2,2,2-Trifluoroacetate (17). ^{1}H NMR (500 MHz, DMSO-d_6, 348 K) δ 7.62 (bs, 1H), 7.35 ($J_{AA'BB'}$ = 8.5 Hz, 2H), 7.30 ($J_{AA'BB'}$ = 8.5 Hz, 2H), 4.05−3.97 (m, 1H), 3.82−3.74 (m, 2H), 3.63−3.54 (m, 2H), 3.30−3.11 (m, 2H), 3.02−2.82 (m, 6H), 2.66 (d, J = 4.7 Hz, 3H), 1.98−1.92 (m, 2H), 1.57−1.47 (m, 2H); ^{1}H NMR (700 MHz, DMSO-d_6 + D_2O, 348 K) δ 7.42−7.32 (m, 4H), 4.37−4.29 (m, 1H), 3.91−3.79 (m, 3H), 3.76−3.63 (m, 3H), 3.33−3.23 (m, 1H), 3.15−3.08 (m, 2H), 3.04−2.93 (m, 2H), 2.54−2.45 (m, 3H), 2.23−2.11 (m, 2H), 1.84−1.66 (m, 2H); ^{13}C NMR (176 MHz, DMSO-d_6) δ 167.8, 134.9, 132.4, 132.0 (2×), 129.1 (2×), 73.2, 64.6, 58.7, 55.9, 45.2, 45.1, 44.7, 39.8, 27.9, 26.0, 25.9, 25.5 (one signal is missing due to overlap); HRMS (ESI) m/z calcd for $C_{20}H_{29}ClN_7O_2$ $[M + H]^+$ 434.2066 found 434.2071.

Protein Expression and Purification. Gene coding human chitotriosidase hCHIT1 catalytic domain (residues 1−386) was cloned into the pCMV2 expression vector. Protein expression was performed in suspension-cultivated mammalian FreeStyle 293-F HEK cells using FectoPro transfection reagent (Polyplus transfection). The secreted protein was purified using three-step protocol. Clarified culture medium was precipitated with ammonium sulfate added to a final saturation of 45%. The precipitate was collected by centrifugation and resuspended in buffer A (20 mM Tris, pH 8.5, 10 mM NaCl, 1 mM DTT). The suspension was concentrated, and the buffer was exchanged to buffer A to remove excess of ammonium sulfate. The material was loaded on a 1 mL Resource Q column (GE Healthcare) equilibrated with buffer A. After loading, the column was washed with buffer A and bounded proteins were eluted with 1 M sodium chloride in buffer A. The flow-through fraction containing hCHIT1 protein was purified by size-exclusion chromatography on a Superdex 200 Increase 10/30 GL (GE Healthcare) column in buffer B (20 mM Tris, pH 8.5, 100 mM NaCl, 1 mM DTT). The protein purity was estimated by SDS−PAGE followed by Coomassie Brilliant Blue staining. The enzyme concentration was determined from the absorption at 280 nm using an UV NanoDrop 1000 spectrophotometer (Thermo Scientific).

Crystallization. For crystallization, the hCHIT1 protein was concentrated to 7.3 mg/mL in buffer B and mixed with **OATD-01** ligand in 1:5 molar ratio. Single crystals were obtained for hCHIT1−**OATD-01** complex mixed with an equal volume of reservoir buffer that contained 0.2 M potassium sodium tartrate (pH 7.2) and 31% (w/v) PEG 3350 using the hanging drop vapor diffusion method at 18 °C. Crystals were cryoprotected in 30% glycerol and flash frozen in liquid nitrogen.

Diffraction Data Collection, Structure Solution, and Refinement. X-ray diffraction data for hCHIT1−**OATD-01** crystals were collected at beamline 14.1 at Berliner Elektronenspeicherring-Gesellschaft für Synchrotronstrahlung (BESSY).[34] The diffraction data were collected to 1.5 Å resolution. Data were processed and scaled with XDS.[49] Phases were determined by molecular replacement using Phaser-MR module in Phenix.[50] The structure of one molecule of hCHIT1 (PDB code 1WBO) was used as the starting model for molecular replacement. Six independent copies of hCHIT1 were found as a MR solution.

The model was improved by manual model building using Coot[51] and refined in Phenix.refine with 5% of unique reflections flagged for R_{free} calculation. The structure of the hCHIT1−**OATD-01** complex was refined with 98.39% residues in the favored region of the Ramachandran plot. X-ray data collection and refinement statistic are summarized in Table 3. Structural analyses and figures were prepared using PyMol (The PyMOL Molecular Graphics System, version 2.2.1, Schrödinger, LLC).

Table 3. Data Collection and Refinement Statistics of hCHIT1−OATD-01 Complex Crystal[a]

Data Collection	
space group	$P\ 2_1\ 2_1\ 2_1$
cell dimensions	
a, *b*, *c* (Å)	87.34, 93.76, 281.68
α, β, γ (deg)	90.00, 90.00, 90.00
resolution (Å)	47.34−1.50 (1.59−1.50)[b]
R_{meas} (%)	7.3 (104.6)[b]
$I/\sigma(I)$	17.04 (1.70)[b]
$CC_{1/2}$[c]	99.9 (61.0)[b]
completeness (%)	99.6 (97.7)[b]
Refinement	
unique reflections	368652
R_{work}/R_{free} (%)	12.3/16.8
number of atoms	20052
protein	17508
ligand ion	162 6
water	2370
B factor	23.6
protein	21.3
ligand/ion	18.1
water	41.0
rms deviation	
bond length (Å)	0.0133
bond angle (deg)	1.14

[a]The data collection statistics are based on a single crystal. [b]Values in parentheses are for highest-resolution shell. [c]$CC_{1/2}$, correlation coefficient between the average intensities in two parts of the unmerged data, each with a random half of the measurements of each unique reflection.

Enzymatic Assays. Determination of IC_{50} toward human and mouse AMCase and human and mouse CHIT1 was done as described previously.[39]

In Vivo Studies. The pharmacokinetics studies were performed in accordance with protocols by the Institute for Animal Care and Use Committee and were approved by Warsaw Local Ethics Committee for Animal Experimentation (Approvals 79/2015, 82/2015, 452/2017), Poland. The animals used in the bleomycin-induced pulmonary fibrosis model were cared for following guidelines Act on Welfare and Management of Animals, Standards Relating to the Care and Management of Laboratory Animals and Relief of Pain, and Guidelines for Proper Conduct of Animal Experiments, Japan.

Pharmacokinetics Measurements in Mice. The PK properties of **OATD-01** were measured in female BALB/c mice following single intravenous bolus (3 mg/kg) or oral (10 mg/kg) administration. Compound **9** (**OATD-01**) was prepared in a in 20% solutol/4% glucose in water vehicle for intravenous bolus and oral administrations at 5 mL/kg, respectively, and administered to 2 mice/group per time point with samples collected up to 24 h after dose. Blood collection was performed by cardiac puncture under anesthesia with sampling of blood into K_2EDTA anticoagulant tubes, followed by centrifugation to obtain plasma. Samples were stored frozen at −80 °C or lower prior to compound extraction and LC−MS/MS analysis. Pharmacokinetic parameters of compound **OATD-01** in mice were calculated by standard noncompartmental modeling from the systemic plasma concentration−time profile.

Pharmacokinetics Measurements in Rats. The PK properties of **OATD-01** were evaluated in male Sprague-Dawley (SD) rats

https://dx.doi.org/10.1021/acs.jmedchem.0c01179
J. Med. Chem. XXXX, XXX, XXX−XXX

following single intravenous bolus (2 mg/kg) or oral (6 mg/kg) administration. **OATD-01** was prepared in a 10% ethanol/10% solutol in water vehicle for intravenous bolus and oral administrations at 1.5 mL/kg or 5 mL/kg, respectively. Blood collection was performed at 5 min (iv only), 15 min (iv only), 30 min, 2 h, 4 h, 6 h, 12 h, and 24 h after **OATD-01** administration ($n = 2$) serially from same animal by tail vein puncture without anesthesia. Blood was collected into K_2EDTA anticoagulant tubes followed by centrifugation to obtain plasma. Plasma samples were snap frozen and stored at −80 °C or lower prior to compound extraction and LC−MS/MS analysis. Pharmacokinetic parameters of **OATD-01** in rats were calculated by standard noncompartmental modeling from the systemic plasma concentration−time profile.

Pharmacokinetics Measurements in Dogs. The PK properties of **OATD-01** were evaluated in male Beagle dogs following single intravenous bolus (3 mg/kg) or oral (10 mg/kg) administration. **OATD-01** was prepared in a 5% aqueous glucose vehicle for intravenous bolus and oral administrations at 0.75 mL/kg or 2.5 mL/kg, respectively. Blood collection was performed at 5 min, 15 min, 30 min, 1 h, 2 h, 4 h, 8 h, and 24 h after dose of **OATD-01** administration, serially from same animal by jugular vein puncture without anesthesia. Blood was collected into sodium heparin anticoagulant tubes followed by centrifugation to obtain plasma. The concentrations of **OATD-01** in dog plasma after extraction were determined by LC−MS/MS. Pharmacokinetic parameters were calculated by standard noncompartmental modeling from the systemic plasma concentration−time profile.

PK/PD Study of OATD-01 (9) in Mice. The PK/PD properties of compound **OATD-01** were evaluated in female C57BL/6N mice (Charles River, Germany) following single (q.d.) and double (b.i.d., interval 8 h) dose of **OATD-01** in 0.5% carboxymethyl cellulose (CMC) administered by oral gavage at 30 mg/kg/dose. A control group received vehicle only. At the defined time-points up to 24 h after last compound administration, mice were preanesthetized with isoflurane, euthanized by overdosing of pentobarbital and blood was collected to EDTA-coated tubes, mixed, and centrifuged 2000*g* for 10 min in 4 °C. The collected plasma was stored in −80 °C until analysis. The perfused lungs were homogenized using bead tissue homogenizer (Bertin Instruments) in 10% ethanol, centrifuged, and the supernatants were collected and stored in −80 °C until analysis. **OATD-01** concentrations in plasma and tissue homogenate were assayed by LC−MS/MS. Chitinolytic activity (PD parameter) in plasma and tissue homogenates was measured as described previously.[39]

Bleomycin-Induced Model of Pulmonary Fibrosis. The study applying bleomycin-induced pulmonary fibrosis model in mice was performed at SMC Laboratories, Inc., Tokyo, Japan. On day 0, 60 mice were anesthetized with pentobarbital sodium (Kyoritsu Seiyaku, Japan) and intratracheally administered with bleomycin (lot no. 261810, Nippon Kayaku, Japan) in saline at a dose of 3 mg/kg, in a volume of 50 μL per animal using a Microsprayer (Penn-Century, USA). The mice were transferred to a clean cage (resting cage) and kept until recovery from anesthesia. The bleomycin administration took place on two separate days, with equal numbers of mice assigned to each day. Control mice were intratracheally administered with saline, instead of the bleomycin, and served as the sham-control group. In each slot, bleomycin-induced pulmonary fibrosis model mice were divided into 5 groups of 6 mice based on the body weight changes on the day before the start of treatment at day 7. **OATD-01** and nintedanib were prepared in 0.5% carboxymethyl cellulose solution and administered orally in a volume of 10 mL/kg. **OATD-01** was administered at two doses 30 and 100 mg/kg q.d., while nintedanib was administered at a reference dose of 100 mg/kg q.d.

Chitinolytic Activity in Plasma. The plasma samples were stored at −80 °C prior to measurement of the chitinolytic activity in these samples as described previously.[39]

Histopathological Analysis of Pulmonary Fibrosis. Right lung tissues prefixed in 10% neutral buffered formalin were embedded in paraffin and sectioned at 4 μm. For fibrosis analysis, the sections were stained with Masson's trichrome kit (Sigma, USA) according to the manufacturer's instructions. The degree of pulmonary fibrosis was evaluated using the Ashcroft score[47,48] for the semiquantitative histological analysis.

■ ASSOCIATED CONTENT

Supporting Information

The Supporting Information is available free of charge at https://pubs.acs.org/doi/10.1021/acs.jmedchem.0c01179.

Molecular formula strings and some data (XLS)

Permeability and physicochemical properties of **OATD-01**; CYPs and transporters inhibition data; superimposition of the active site residues in hCHIT1 complexed to **OATD-01** and **OAT-177**; PK profiles of compounds **11** and **15**−**17**; experimental procedures for compounds **5**, **7**, **8**, **15**−**17**; ^{1}H NMR spectra of compounds **5**−**17**; HPLC profile of compounds **3**−**17** (PDF)

Accession Codes

Atomic coordinates and structure factors for the reported crystal structure have been deposited in the Protein Data Bank (PDB code 6ZE8) and will be released upon publication.

■ AUTHOR INFORMATION

Corresponding Author

Adam Golebiowski − *OncoArendi Therapeutics SA, 02-089 Warsaw, Poland*; orcid.org/0000-0001-5960-2995; Phone: +48 (22) 552 67 24; Email: a.golebiowski@oncoarendi.com

Authors

Robert Koralewski − *OncoArendi Therapeutics SA, 02-089 Warsaw, Poland*

Barbara Dymek − *OncoArendi Therapeutics SA, 02-089 Warsaw, Poland*

Marzena Mazur − *OncoArendi Therapeutics SA, 02-089 Warsaw, Poland*

Piotr Sklepkiewicz − *OncoArendi Therapeutics SA, 02-089 Warsaw, Poland*

Sylwia Olejniczak − *OncoArendi Therapeutics SA, 02-089 Warsaw, Poland*

Wojciech Czestkowski − *OncoArendi Therapeutics SA, 02-089 Warsaw, Poland*

Krzysztof Matyszewski − *OncoArendi Therapeutics SA, 02-089 Warsaw, Poland*

Gleb Andryianau − *OncoArendi Therapeutics SA, 02-089 Warsaw, Poland*

Piotr Niedziejko − *OncoArendi Therapeutics SA, 02-089 Warsaw, Poland*

Michal Kowalski − *OncoArendi Therapeutics SA, 02-089 Warsaw, Poland*

Mariusz Gruza − *OncoArendi Therapeutics SA, 02-089 Warsaw, Poland*

Bartłomiej Borek − *OncoArendi Therapeutics SA, 02-089 Warsaw, Poland*

Karol Jedrzejczak − *OncoArendi Therapeutics SA, 02-089 Warsaw, Poland*

Agnieszka Bartoszewicz − *OncoArendi Therapeutics SA, 02-089 Warsaw, Poland*

Elżbieta Pluta − *OncoArendi Therapeutics SA, 02-089 Warsaw, Poland*

Aleksandra Rymaszewska − *OncoArendi Therapeutics SA, 02-089 Warsaw, Poland*

https://dx.doi.org/10.1021/acs.jmedchem.0c01179
J. Med. Chem. XXXX, XXX, XXX−XXX

Magdalena Kania − *OncoArendi Therapeutics SA, 02-089 Warsaw, Poland*
Tomasz Rejczak − *OncoArendi Therapeutics SA, 02-089 Warsaw, Poland*
Sylwia Piasecka − *OncoArendi Therapeutics SA, 02-089 Warsaw, Poland*
Michal Mlacki − *OncoArendi Therapeutics SA, 02-089 Warsaw, Poland*
Marcin Mazurkiewicz − *OncoArendi Therapeutics SA, 02-089 Warsaw, Poland*
Michał Piotrowicz − *OncoArendi Therapeutics SA, 02-089 Warsaw, Poland;* orcid.org/0000-0001-7214-858X
Magdalena Salamon − *OncoArendi Therapeutics SA, 02-089 Warsaw, Poland*
Agnieszka Zagozdzon − *OncoArendi Therapeutics SA, 02-089 Warsaw, Poland*
Agnieszka Napiorkowska-Gromadzka − *Structural Biology Center, International Institute of Molecular and Cell Biology, 02-109 Warsaw, Poland*
Aneta Bartlomiejczak − *Structural Biology Center, International Institute of Molecular and Cell Biology, 02-109 Warsaw, Poland*
Witold Mozga − *OncoArendi Therapeutics SA, 02-089 Warsaw, Poland*
Paweł Dobrzański − *OncoArendi Therapeutics SA, 02-089 Warsaw, Poland*
Karolina Dzwonek − *OncoArendi Therapeutics SA, 02-089 Warsaw, Poland*
Jakub Golab − *OncoArendi Therapeutics SA, 02-089 Warsaw, Poland; Department of Immunology, Medical University of Warsaw, 02-097 Warsaw, Poland*
Marcin Nowotny − *Structural Biology Center, International Institute of Molecular and Cell Biology, 02-109 Warsaw, Poland;* orcid.org/0000-0001-8632-0977
Jacek Olczak − *OncoArendi Therapeutics SA, 02-089 Warsaw, Poland;* orcid.org/0000-0001-9932-2373

Complete contact information is available at: https://pubs.acs.org/10.1021/acs.jmedchem.0c01179

Author Contributions

The manuscript was written through contributions of all authors. All authors have given approval to the final version of the manuscript.

Notes

The authors declare the following competing financial interest(s): Some of the authors are current employees of OncoArendi Therapeutics SA and own company stocks.

■ ACKNOWLEDGMENTS

Studies were supported by two projects: (1) "Development of a first-in-class small molecule drug candidate for treatment of idiopathic pulmonary fibrosis through chitotriosidase inhibition" (Grant POIR.01.01.01-00-0551/15), acronym IPF, and (2) "Preclinical research and clinical trials of a first-in class development candidate in therapy of asthma and inflammatory bowel disease" (Grant POIR.01.01.01- 00-0168/15), acronym IBD. Both were cofunded by the National Centre for Research and Development in the framework of European Funds Smart Growth.

■ ABBREVIATIONS USED

AMCase, acidic mammalian chitinase; hAMCase, human acidic mammalian chitinase; mAMCase, mouse acidic mammalian chitinase; CHIT1, chitotriosidase; hCHIT1, human chitotriosidase; mCHIT1, mouse chitotriosidase; IL-13, interleukin 13; Th2, type 2 helper T cell; TBTU, *N,N,N′,N′*-tetramethyl-*O*-(benzotriazol-1-yl)uronium tetrafluoroborate; DIPEA, *N,N*-diisopropylethylamine; V_{ss}, steady-state volume of distribution; CL, clearance; AUC_{0-inf}, area under the curve; C_{max}, peak plasma concentration of a drug after administration; T_{max}, time to reach C_{max}; BAL, bronchoalveolar lavage

■ REFERENCES

(1) Lee, C. G.; Da Silva, C. A.; Dela Cruz, C. S.; Ahangari, F.; Ma, B.; Kang, M. J.; He, C. H.; Takyar, S.; Elias, J. A. Role of chitin and chitinase/chitinase-like proteins in inflammation, tissue remodeling, and injury. *Annu. Rev. Physiol.* **2011**, *73*, 479−501.
(2) Mack, I.; Hector, A.; Ballbach, M.; Kohlhaufl, J.; Fuchs, K. J.; Weber, A.; Mall, M. A.; Hartl, D. The role of chitin, chitinases, and chitinase-like proteins in pediatric lung diseases. *Mol. Cell Pediatr.* **2015**, *2*, 3.
(3) van Eijk, M.; van Roomen, C. P.; Renkema, G. H.; Bussink, A. P.; Andrews, L.; Blommaart, E. F.; Sugar, A.; Verhoeven, A. J.; Boot, R. G.; Aerts, J. M. Characterization of human phagocyte-derived chitotriosidase, a component of innate immunity. *Int. Immunol.* **2005**, *17*, 1505−1512.
(4) Boot, R. G.; Blommaart, E. F.; Swart, E.; Ghauharali-Van der Vlugt, K.; Bijl, N.; Moe, C.; Place, A.; Aerts, J. M. Identification of a novel acidic mammalian chitinase distinct from chitotriosidase. *J. Biol. Chem.* **2001**, *276*, 6770−6778.
(5) Fadel, F.; Zhao, Y.; Cousido-Siah, A.; Ruiz, F. X.; Mitschler, A.; Podjarny, A. X-ray crystal structure of the full length human chitotriosidase (CHIT1) reveals features of its chitin binding domain. *PLoS One* **2016**, *11*, No. e0154190.
(6) Garth, J. M.; Mackel, J. J.; Reeder, K. M.; Blackburn, J. P.; Dunaway, C. W.; Yu, Z.; Matalon, S.; Fitz, L.; Steele, C. Acidic mammalian chitinase negatively affects immune responses during acute and chronic Aspergillus fumigatus exposure. *Infect. Immun.* **2018**, *86*, e00944-17.
(7) Yang, C. J.; Liu, Y. K.; Liu, C. L.; Shen, C. N.; Kuo, M. L.; Su, C. C.; Tseng, C. P.; Yen, T. C.; Shen, C. R. Inhibition of acidic mammalian chitinase by RNA interference suppresses ovalbumin-sensitized allergic asthma. *Hum. Gene Ther.* **2009**, *20*, 1597−1606.
(8) Zhu, Z.; Zheng, T.; Homer, R. J.; Kim, Y. K.; Chen, N. Y.; Cohn, L.; Hamid, Q.; Elias, J. A. Acidic mammalian chitinase in asthmatic Th2 inflammation and IL-13 pathway activation. *Science* **2004**, *304*, 1678−1682.
(9) Agapov, E.; Battaile, J. T.; Tidwell, R.; Hachem, R.; Patterson, G. A.; Pierce, R. A.; Atkinson, J. J.; Holtzman, M. J. Macrophage chitinase 1 stratifies chronic obstructive lung disease. *Am. J. Respir. Cell Mol. Biol.* **2009**, *41*, 379−384.
(10) Cho, S. J.; Weiden, M. D.; Lee, C. G. Chitotriosidase in the pathogenesis of inflammation, interstitial lung diseases and COPD. *Allergy, Asthma Immunol. Res.* **2015**, *7*, 14−21.
(11) Di Rosa, M.; De Gregorio, C.; Malaguarnera, G.; Tuttobene, M.; Biazzo, F.; Malaguarnera, L. Evaluation of AMCase and CHIT-1 expression in monocyte macrophages lineage. *Mol. Cell. Biochem.* **2013**, *374*, 73−80.
(12) Seibold, M. A.; Donnelly, S.; Solon, M.; Innes, A.; Woodruff, P. G.; Boot, R. G.; Burchard, E. G.; Fahy, J. V. Chitotriosidase is the primary active chitinase in the human lung and is modulated by genotype and smoking habit. *J. Allergy Clin. Immunol.* **2008**, *122*, 944−950.
(13) Li, X.; Zhu, L.; Wang, B.; Yuan, M.; Zhu, R. Drugs and targets in fibrosis. *Front. Pharmacol.* **2017**, *8*, 855.
(14) Malaguarnera, L.; Di Rosa, M.; Zambito, A. M.; dell'Ombra, N.; Di Marco, R.; Malaguarnera, M. Potential role of chitotriosidase gene

in nonalcoholic fatty liver disease evolution. *Am. J. Gastroenterol.* **2006**, *101*, 2060−2069.
(15) Malaguarnera, L.; Di Rosa, M.; Zambito, A. M.; dell'Ombra, N.; Nicoletti, F.; Malaguarnera, M. Chitotriosidase gene expression in Kupffer cells from patients with non-alcoholic fatty liver disease. *Gut* **2006**, *55*, 1313−1320.
(16) Lee, C. G.; Herzog, E. L.; Ahangari, F.; Zhou, Y.; Gulati, M.; Lee, C. M.; Peng, X.; Feghali-Bostwick, C.; Jimenez, S. A.; Varga, J.; Elias, J. A. Chitinase 1 is a biomarker for and therapeutic target in scleroderma-associated interstitial lung disease that augments TGF-beta1 signaling. *J. Immunol.* **2012**, *189*, 2635−2644.
(17) Ramanathan, R.; Kohli, A.; Ingaramo, M. C.; Jain, A.; Leng, S. X.; Punjabi, N. M.; Walston, J. D.; Fedarko, N. S. Serum chitotriosidase, a putative marker of chronically activated macrophages, increases with normal aging. *J. Gerontol., Ser. A* **2013**, *68*, 1303−1309.
(18) James, A. J.; Reinius, L. E.; Verhoek, M.; Gomes, A.; Kupczyk, M.; Hammar, U.; Ono, J.; Ohta, S.; Izuhara, K.; Bel, E.; Kere, J.; Soderhall, C.; Dahlen, B.; Boot, R. G.; Dahlen, S. E. Increased YKL-40 and chitotriosidase in asthma and chronic obstructive pulmonary disease. *Am. J. Respir. Crit. Care Med.* **2016**, *193*, 131−142.
(19) Kim, L. K.; Morita, R.; Kobayashi, Y.; Eisenbarth, S. C.; Lee, C. G.; Elias, J.; Eynon, E. E.; Flavell, R. A. AMCase is a crucial regulator of type 2 immune responses to inhaled house dust mites. *Proc. Natl. Acad. Sci. U. S. A.* **2015**, *112*, E2891−2899.
(20) Mazur, M.; Olczak, J.; Olejniczak, S.; Koralewski, R.; Czestkowski, W.; Jedrzejczak, A.; Golab, J.; Dzwonek, K.; Dymek, B.; Sklepkiewicz, P. L.; Zagozdzon, A.; Noonan, T.; Mahboubi, K.; Conway, B.; Sheeler, R.; Beckett, P.; Hungerford, W. M.; Podjarny, A.; Mitschler, A.; Cousido-Siah, A.; Fadel, F.; Golebiowski, A. Targeting acidic mammalian chitinase is effective in animal model of asthma. *J. Med. Chem.* **2018**, *61*, 695−710.
(21) Bargagli, E.; Margollicci, M.; Luddi, A.; Nikiforakis, N.; Perari, M. G.; Grosso, S.; Perrone, A.; Rottoli, P. Chitotriosidase activity in patients with interstitial lung diseases. *Respir. Med.* **2007**, *101*, 2176−2181.
(22) Bargagli, E.; Bennett, D.; Maggiorelli, C.; Di Sipio, P.; Margollicci, M.; Bianchi, N.; Rottoli, P. Human chitotriosidase: a sensitive biomarker of sarcoidosis. *J. Clin. Immunol.* **2013**, *33*, 264−270.
(23) Bargagli, E.; Margollicci, M.; Nikiforakis, N.; Luddi, A.; Perrone, A.; Grosso, S.; Rottoli, P. Chitotriosidase activity in the serum of patients with sarcoidosis and pulmonary tuberculosis. *Respiration* **2007**, *74*, 548−552.
(24) Aminuddin, F.; Akhabir, L.; Stefanowicz, D.; Pare, P. D.; Connett, J. E.; Anthonisen, N. R.; Fahy, J. V.; Seibold, M. A.; Burchard, E. G.; Eng, C.; Gulsvik, A.; Bakke, P.; Cho, M. H.; Litonjua, A.; Lomas, D. A.; Anderson, W. H.; Beaty, T. H.; Crapo, J. D.; Silverman, E. K.; Sandford, A. J. Genetic association between human chitinases and lung function in COPD. *Hum. Genet.* **2012**, *131*, 1105−1114.
(25) Byrne, A. J.; Maher, T. M.; Lloyd, C. M. Pulmonary macrophages: a new therapeutic pathway in fibrosing lung disease? *Trends Mol. Med.* **2016**, *22*, 303−316.
(26) King, T. E., Jr.; Pardo, A.; Selman, M. Idiopathic pulmonary fibrosis. *Lancet* **2011**, *378*, 1949−1961.
(27) Martinez, F. J.; Safrin, S.; Weycker, D.; Starko, K. M.; Bradford, W. Z.; King, T. E., Jr.; Flaherty, K. R.; Schwartz, D. A.; Noble, P. W.; Raghu, G.; Brown, K. K. The clinical course of patients with idiopathic pulmonary fibrosis. *Ann. Intern. Med.* **2005**, *142*, 963−967.
(28) Murray, L. A. Commonalities between the pro-fibrotic mechanisms in COPD and IPF. *Pulm. Pharmacol. Ther.* **2012**, *25*, 276−280.
(29) Reyfman, P. A.; Walter, J. M.; Joshi, N.; Anekalla, K. R.; McQuattie-Pimentel, A. C.; Chiu, S.; Fernandez, R.; Akbarpour, M.; Chen, C. I.; Ren, Z.; Verma, R.; Abdala-Valencia, H.; Nam, K.; Chi, M.; Han, S.; Gonzalez-Gonzalez, F. J.; Soberanes, S.; Watanabe, S.; Williams, K. J. N.; Flozak, A. S.; Nicholson, T. T.; Morgan, V. K.; Winter, D. R.; Hinchcliff, M.; Hrusch, C. L.; Guzy, R. D.; Bonham, C. A.; Sperling, A. I.; Bag, R.; Hamanaka, R. B.; Mutlu, G. M.; Yeldandi, A. V.; Marshall, S. A.; Shilatifard, A.; Amaral, L. A. N.; Perlman, H.; Sznajder, J. I.; Argento, A. C.; Gillespie, C. T.; Dematte, J.; Jain, M.; Singer, B. D.; Ridge, K. M.; Lam, A. P.; Bharat, A.; Bhorade, S. M.; Gottardi, C. J.; Budinger, G. R. S.; Misharin, A. V. Single-cell transcriptomic analysis of human lung provides insights into the pathobiology of pulmonary fibrosis. *Am. J. Respir. Crit. Care Med.* **2019**, *199*, 1517−1536.
(30) Chang; Sharma, L.; Dela Cruz, C. S. Chitotriosidase: a marker and modulator of lung disease. *Eur. Respir. Rev.* **2020**, *29*, 190143.
(31) Przysucha, N.; Gorska, K.; Krenke, R. Chitinases and chitinase-like proteins in obstructive lung diseases - current concepts and potential applications. *Int. J. Chronic Obstruct. Pulm. Dis.* **2020**, *15*, 885−899.
(32) Di Rosa, M.; Mangano, K.; De Gregorio, C.; Nicoletti, F.; Malaguarnera, L. Association of chitotriosidase genotype with the development of non-alcoholic fatty liver disease. *Hepatol. Res.* **2013**, *43*, 267−275.
(33) Wandrer, F.; Han, B.; Liebig, S.; Schlue, J.; Manns, M. P.; Schulze-Osthoff, K.; Bantel, H. Senescence mirrors the extent of liver fibrosis in chronic hepatitis C virus infection. *Aliment. Pharmacol. Ther.* **2018**, *48*, 270−280.
(34) Mueller, U.; Darowski, N.; Fuchs, M. R.; Forster, R.; Hellmig, M.; Paithankar, K. S.; Puhringer, S.; Steffien, M.; Zocher, G.; Weiss, M. S. Facilities for macromolecular crystallography at the Helmholtz-Zentrum Berlin. *J. Synchrotron Radiat.* **2012**, *19*, 442−449.
(35) Hirose, T.; Sunazuka, T.; Omura, S. Recent development of two chitinase inhibitors, Argifin and Argadin, produced by soil microorganisms. *Proc. Jpn. Acad., Ser. B* **2010**, *86*, 85−102.
(36) Cole, D. C.; Olland, A. M.; Jacob, J.; Brooks, J.; Bursavich, M. G.; Czerwinski, R.; DeClercq, C.; Johnson, M.; Joseph-McCarthy, D.; Ellingboe, J. W.; Lin, L.; Nowak, P.; Presman, E.; Strand, J.; Tam, A.; Williams, C. M. M.; Yao, S.; Tsao, D. H. H.; Fitz, L. J. Identification and characterization of acidic mammalian chitinase inhibitors. *J. Med. Chem.* **2010**, *53*, 6122−6128.
(37) Andryianau, G.; Kowalski, M.; Piotrowicz, M. C.; Rajkiewicz, A. A.; Dymek, B.; Sklepkiewicz, P. L.; Pluta, E.; Stefaniak, F.; Czestkowski, W.; Olejniczak, S.; Mazur, M.; Niedziejko, P.; Koralewski, R.; Matyszewski, K.; Gruza, M.; Zagozdzon, A.; Salamon, M.; Rymaszewska, A.; Welzer, M.; Dzwonek, K.; Golab, J.; Olczak, J.; Bartoszewicz, A.; Golebiowski, A. Benzoxazepine-derived selective, orally bioavailable inhibitor of human acidic mammalian chitinase. *ACS Med. Chem. Lett.* **2020**, *11*, 1228−1235.
(38) Mazur, M.; Bartoszewicz, A.; Dymek, B.; Salamon, M.; Andryianau, G.; Kowalski, M.; Olejniczak, S.; Matyszewski, K.; Pluta, E.; Borek, B.; Stefaniak, F.; Zagozdzon, A.; Mazurkiewicz, M.; Koralewski, R.; Czestkowski, W.; Piotrowicz, M.; Niedziejko, P.; Gruza, M. M.; Dzwonek, K.; Golebiowski, A.; Golab, J.; Olczak, J. Discovery of selective, orally bioavailable inhibitor of mouse chitotriosidase. *Bioorg. Med. Chem. Lett.* **2018**, *28*, 310−314.
(39) Mazur, M.; Dymek, B.; Koralewski, R.; Sklepkiewicz, P.; Olejniczak, S.; Mazurkiewicz, M.; Piotrowicz, M.; Salamon, M.; Jedrzejczak, K.; Zagozdzon, A.; Czestkowski, W.; Matyszewski, K.; Borek, B.; Bartoszewicz, A.; Pluta, E.; Rymaszewska, A.; Mozga, W.; Stefaniak, F.; Dobrzanski, P.; Dzwonek, K.; Golab, J.; Golebiowski, A.; Olczak, J. Development of dual chitinase inhibitors as potential new treatment for respiratory system diseases. *J. Med. Chem.* **2019**, *62*, 7126−7145.
(40) Jiang, X.; Kumar, A.; Motomura, Y.; Liu, T.; Zhou, Y.; Moro, K.; Zhang, K. Y. J.; Yang, Q. A Series of compounds bearing a dipyrido-pyrimidine scaffold acting as novel human and insect pest chitinase inhibitors. *J. Med. Chem.* **2020**, *63*, 987−1001.
(41) Piper, D. R.; Duff, S. R.; Eliason, H. C.; Frazee, W. J.; Frey, E. A.; Fuerstenau-Sharp, M.; Jachec, C.; Marks, B. D.; Pollok, B. A.; Shekhani, M. S.; Thompson, D. V.; Whitney, P.; Vogel, K. W.; Hess, S. D. Development of the predictor HERG fluorescence polarization assay using a membrane protein enrichment approach. *Assay Drug Dev. Technol.* **2008**, *6*, 213−223.

https://dx.doi.org/10.1021/acs.jmedchem.0c01179
J. Med. Chem. XXXX, XXX, XXX−XXX

(42) Commercially available assay. https://www.eurofinsdiscoveryservices.com/catalogmanagement/viewitem/DATRat-Dopamine-Transporter-Functional-Antagonist-Uptake-Assay-Cerep/394 (accessed Mar 19, 2019).
(43) Kuntz, K. W.; Campbell, J. E.; Keilhack, H.; Pollock, R. M.; Knutson, S. K.; Porter-Scott, M.; Richon, V. M.; Sneeringer, C. J.; Wigle, T. J.; Allain, C. J.; Majer, C. R.; Moyer, M. P.; Copeland, R. A.; Chesworth, R. The Importance of being Me: magic methyls, methyltransferase inhibitors, and the discovery of tazemetostat. *J. Med. Chem.* **2016**, *59*, 1556−1564.
(44) Leung, C. S.; Leung, S. S.; Tirado-Rives, J.; Jorgensen, W. L. Methyl effects on protein-ligand binding. *J. Med. Chem.* **2012**, *55*, 4489−4500.
(45) Stumpfe, D.; Hu, Y.; Dimova, D.; Bajorath, J. Recent progress in understanding activity cliffs and their utility in medicinal chemistry. *J. Med. Chem.* **2014**, *57*, 18−28.
(46) Sammons, M.; Jennings, S. M.; Herr, M.; Hulford, C. A.; Wei, L.; Hallissey, J. F.; Kiser, E. J.; Wright, S. W.; Piotrowski, D. W. Synthesis of a cis 2,5-disubstituted morpholine by de-epimerization: application to the multigram scale synthesis of a mineralocorticoid antagonist. *Org. Process Res. Dev.* **2013**, *17*, 934−939.
(47) Ashcroft, T.; Simpson, J. M.; Timbrell, V. Simple method of estimating severity of pulmonary fibrosis on a numerical scale. *J. Clin. Pathol.* **1988**, *41*, 467−470.
(48) Hubner, R. H.; Gitter, W.; El Mokhtari, N. E.; Mathiak, M.; Both, M.; Bolte, H.; Freitag-Wolf, S.; Bewig, B. Standardized quantification of pulmonary fibrosis in histological samples. *BioTechniques* **2008**, *44*, 507−517.
(49) Kabsch, W. XDS. *Acta Crystallogr., Sect. D: Biol. Crystallogr.* **2010**, *66*, 125−132.
(50) Adams, P. D.; Afonine, P. V.; Bunkoczi, G.; Chen, V. B.; Davis, I. W.; Echols, N.; Headd, J. J.; Hung, L. W.; Kapral, G. J.; Grosse-Kunstleve, R. W.; McCoy, A. J.; Moriarty, N. W.; Oeffner, R.; Read, R. J.; Richardson, D. C.; Richardson, J. S.; Terwilliger, T. C.; Zwart, P. H. PHENIX: a comprehensive Python-based system for macromolecular structure solution. *Acta Crystallogr., Sect. D: Biol. Crystallogr.* **2010**, *66*, 213−221.
(51) Emsley, P.; Lohkamp, B.; Scott, W. G.; Cowtan, K. Features and development of Coot. *Acta Crystallogr., Sect. D: Biol. Crystallogr.* **2010**, *66*, 486−501.

https://dx.doi.org/10.1021/acs.jmedchem.0c01179
J. Med. Chem. XXXX, XXX, XXX−XXX